Carbazole-based colorimetric anion sensors

Krystyna Maslowska-Jarzyna [1], Maria L. Korczak [1] Jakub A. Wagner [1] and Michał J. Chmielewski [1,*]

[1] Faculty of Chemistry, Biological and Chemical Research Centre, University of Warsaw, Żwirki i Wigury 101, 02-089 Warsaw, Poland; kmaslowska@chem.uw.edu.pl, ml.korczak@student.uw.edu.pl, ja.wagner@student.uw.edu.pl;

* Correspondence: mchmielewski@chem.uw.edu.pl

Abstract: Endowed with strong carbazole chromophore and fluorophore as well as with powerful and convergent hydrogen bond donors, 1,8-diaminocarbazoles are amongst the most attractive and synthetically versatile building blocks for the construction of anion receptors, sensors and transporters. Aiming at the development of carbazole-based colorimetric anion sensors, we describe here the synthesis of 1,8-diaminocarbazoles substituted with strongly electron-withdrawing substituents: 3,6-dicyano and 3,6-dinitro. Both of these precursors were subsequently converted into model diamide receptors. Anion binding studies revealed that the new receptors show greatly enhanced anion affinity, but also significantly increased acidity. We found also that rear substitution of 1,8-diamidocarbazole with two nitro groups shifts its absorption spectrum to the visible region and converts receptor into colorimetric anion sensor. The new sensor produces vivid changes in colour and fluorescence upon addition of basic anions in wet DMSO, but is poorly selective: due to its greatly enhanced acidity, for most anions the dominant receptor-anion interaction is proton transfer and, accordingly, similar changes in colour can be observed for every basic anion. The highly acidic and strongly binding receptors developed in this study may find applications in organocatalysis or in pH-switchable anion transport through lipophilic membranes.

Keywords: supramolecular chemistry, anion recognition, anion receptors, anion sensors, colorimetric sensors

1. Introduction

Molecules that selectively change their colour or fluorescence in response to anionic species are highly appealing for applications in many branches of science, industry and medicine [1]. Such changes may be induced by hydrogen bonding interactions with anions, especially in cases where hydrogen bond donors are directly coupled with the receptor's chromophores or fluorophores [2-7]. If these changes are sufficiently strong and affect visible part of the spectra, they may even be detected by naked eye [2]. Significant research efforts have therefore been directed towards the development of colorimetric and fluorescent anion sensors based on hydrogen bond donating receptors [8-9].

One particularly appealing building block for the development of colorimetric and fluorescent anion sensors is 1,8-diaminocarbazole [10]. It combines several attractive features, such as the presence of a strong carbazole chromophore and fluorophore directly coupled with anion binding sites, strong hydrogen bond donor – carbazole NH, rigid skeleton that facilitates preorganization of auxiliary hydrogen bond donors and the ease of synthesis and derivatization. Diaminocarbazole-based receptors show particularly high affinity towards oxyanions (carboxylates, phosphates and sulphates) [3,11-24] and some of them are also very active anion transporters [22,25-26].

However, carbazole has negligible absorption in the visible part of the spectrum and accordingly, in the absence of other chromophores, diaminocarbazole-based receptors are colourless. It has been shown that substitution of positions 3 and 6 with mildly electron-withdrawing chlorine atoms shifts the UV spectrum of diamidocarbazoles almost to the verge of the visible region and, at the same time, increase their anion binding constants by up to an order of magnitude [22]. We hypothesized therefore, that more strongly electron-withdrawing substituents could turn such receptors into colorimetric anion sensors and, at the same time, enhance their binding constants even more significantly. In this paper we describe the synthesis and anion sensing properties of 3,6-dicyano- and 3,6-dinitro- substituted carbazole receptors **3** and **4** and compare them with the previously described [19,22] 3,6-unsubstituted and 3,6-dichlorosubstituted receptors **1** and **2** (Figure 1).

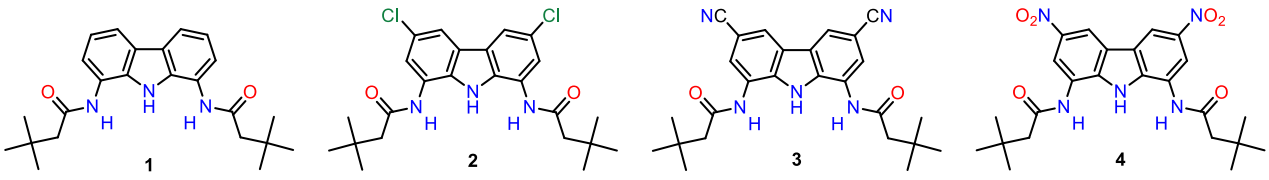

Figure 1. Model receptors used in this study.

2. Results and discussion

2.1. Synthesis

Carbazole is electron rich and readily undergoes electrophilic aromatic substitution in positions 3 and 6. Only after these positions are blocked by, for example, chlorination, nitration smoothly goes into positions 1 and 8 giving the desired dinitro derivative: 3,6-dichloro-1,8-dinitrocarbazole **7** [27]. Subsequent reduction yields either 1,8-diamino-3,6-dichlorocarbazole **8** [22] or 1,8-diaminocarbazole **9** [28], depending upon particular reagents and conditions. The two diamines have already been used for the synthesis of a variety of anion receptors, including amides, thioamides, sulfonamides and ureas [17-18,20,26]. Previously, we used them also for the synthesis of model receptors **1** and **2** (Scheme 1) [19,22]:

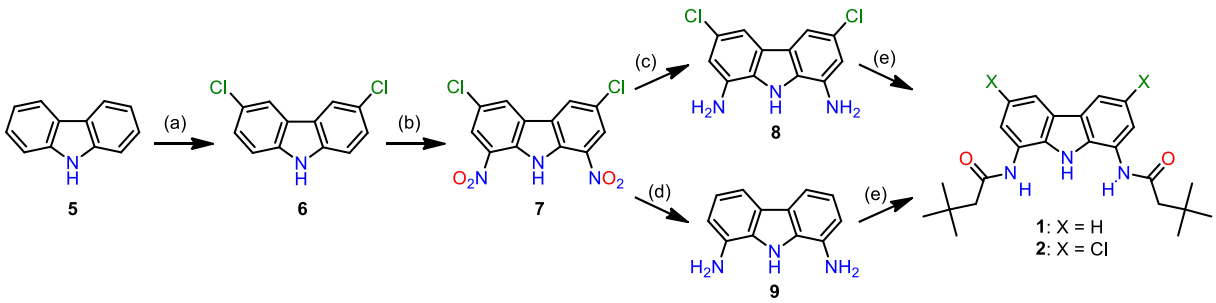

Scheme 1. The synthesis of receptors **1** and **2** [19,22]. (a) SO_2Cl_2, CH_2Cl_2, RT, 60%. (b) HNO_3 (100%), Ac_2O/AcOH, 1 °C to 110 °C, 73%. (c) H_2 (balloon), 5%Pt(S)/C (cat.), CH_3CN, RT, 90%. (d) NH_2NH_2, 10%Pd/C (cat.), EtOH, reflux, 6 h, 75%. (e) $(CH_3)_3CH_2COCl$, Et_3N, CH_3CN, RT, 40–88%.

Similar strategy has been adopted in the present work for the synthesis of 3,6-dicyano substituted receptor **3** (Scheme 2).

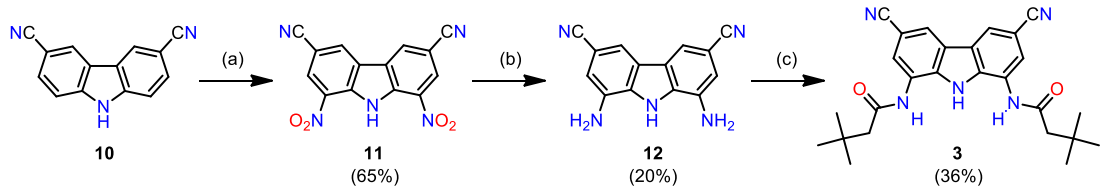

Scheme 2. The synthesis of receptor **3**. (a) HNO_3 (100%), Ac_2O/AcOH, 1 °C to 110 °C, 12 h, 66%; (b) $NH_2NH_2{\cdot}H_2O$, $FeSO_4{\cdot}7H_2O$, EtOH, reflux, 48 h, 20%; (c) $(CH_3)_3CH_2COCl$, DMA, RT, 24 h, 36%.

The synthesis starts from 3,6-dicyanocarbazole **10**, which is easily available in two steps from carbazole [29]. Nitration of **10** with acetyl nitrate (formed *in situ* from 100% nitric acid and acetic anhydride), under conditions optimized previously for the 3,6-dichlorocarbazole **6** [27], led to 2:1 mixture of mononitro- and dinitro- derivatives **14** and **11** (Scheme 3). This is apparently due to the stronger deactivation of the carbazole core by the -CN groups. On the other hand, much harsher conditions, such as boiling in the HNO_3/Ac_2O/AcOH mixture or using a mixture of concentrated sulfuric and nitric acids, lead to the extensive formation of degradation products or the formation of 1,3,6,8-tetranitrocarbazole **15**, respectively. The reaction conditions were therefore carefully optimized, with particular emphasis on the reaction temperature and the substrate/HNO_3 and HNO_3/Ac_2O ratios.

Surprisingly, at 50 °C the main product turned out to be *N,N'*-bis(3,6-dicyanocarbazole) **13**, with only traces of nitration products present in the reaction mixture after 40 h (Scheme 3). Heating at 70 °C for 40 h led to the mixture of biscarbazole **13**, 3,6-dicyano-1-nitrocarbazole **14** and small amounts of the desired 3,6-dicyano-1,8-dinitrocarbazole **11**. Further increase of the reaction temperature to 90 °C resulted in the complete disappearance of **13** and preferential formation of the desired dinitrocarbazole **11**. Unfortunately, however, significant amounts of the mononitro derivative **14** were still present in the reaction mixture under these conditions. The two nitro compounds are very difficult to separate and therefore the reaction conditions had to be optimized further to completely eliminate the formation of this by-product. To our delight, at 110 °C very clean formation of the dinitro product was observed, somewhat surprisingly given that already at 118 °C (the boiling point of the mixture) extensive decomposition takes place. Also, the nitrating

reagent – acetyl nitrate – decomposes more and more rapidly at temperatures above 60 °C [30]. As a consequence, the nitration at 110 °C requires large excess of 100% HNO_3 and is quite capricious.

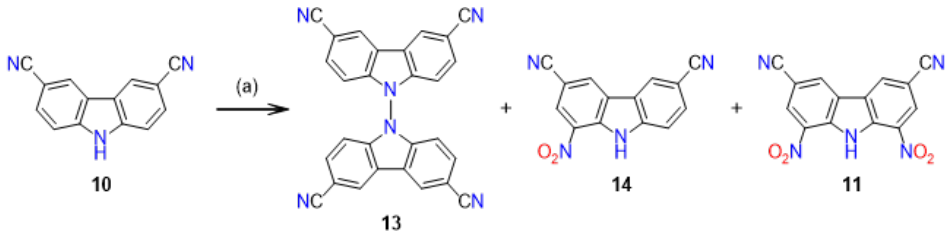

Scheme 3. Nitration of 3,6-dicyanocarbazole **10**. (a) HNO_3 (100%)/Ac_2O/AcOH, various temperatures.

To circumvent the extensive decomposition of acetyl nitrate, the nitric acid was added in small portions and the mixture was cooled down prior to each addition. Also, the reaction was monitored by ^1H NMR and continued until all the signals from **14** disappeared. Using these precautions, clean formation of **11** can be accomplished. The product precipitates from the reaction mixture in an almost pure form and can be obtained in 66% yield after simple filtration and washing with diethyl ether. It is worth noting that the 3,6-dicyano-1,8-dinitrocarbazole **11** might be a very useful synthon, because it bears as many as 5 amino group equivalents on a small, rigid core and is available in just three steps from the very cheap carbazole.

Selective reduction of the two nitro groups of **11** proved difficult, however, and gave the desired 1,8-diamino-3,6-dicyanocarbazole **12** in just 20% yield (not optimized). Also, the final acylation of **12** with *t*-butylacetyl chloride was more problematic then in the case of receptors **1** and **2**, because the strongly electron withdrawing -CN groups make **3** prone to over-acylation, which leads to a very difficult to separate imide impurity. It was necessary therefore to develop a different protocol for this reaction. It turned out that in the absence of any base and in dimethylacetamide as a solvent the formation of the imide is suppressed, and the desired receptor **3** can be obtained in pure form, although in just 36% yield (Scheme 2).

Extension of the same synthetic strategy to the synthesis of receptor **4** seemed to be problematic because it requires selective reduction of only two of the four nitro groups of 1,3,6,8-tetranitrocarbazole **15** (Scheme 4). However, since the tetranitrocarbazole **15** is commercially available, we took up the challenge and, after some experimentation, found the appropriate reagent and conditions for this transformation. It turned out that 1,8-diamino-3,6-dinitrocarbazole **16** can be selectively obtained in 78% yield using hydrazine hydrate as reductor and iron(II) sulfate as catalyst [31]. This finding opens a very convenient access to another very attractive synthon, which also bears 5 amino group equivalents on a single carbazole core.

Acylation of **16** with *t*-butylacetyl chloride under standard conditions (AN, Et_3N) also produces a difficult to separate imide impurity. As in the case of **3** described above, elimination of any base and application of dimethylacetamide as solvent suppressed the over-acylation and yielded pure receptor **4** in 58 % yield (Scheme 4).

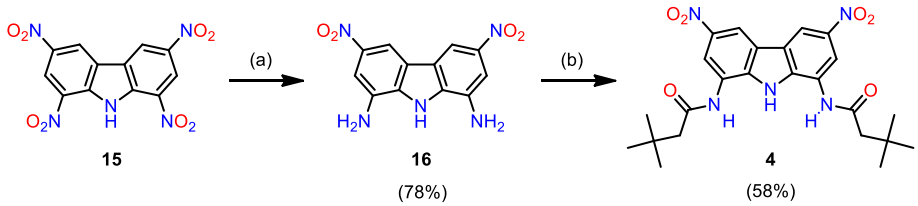

Scheme 4. Synthetic pathway leading to the receptor **4**. Isolated yields are given in parentheses. (a) $NH_2NH_2{\cdot}H_2O$, $FeSO_4{\cdot}7H_2O$, EtOH, reflux, 20h; (b) 3,3-dimethylbutyryl chloride, DMA, RT, 20h.

2.2. Anion recognition studies

The anion binding studies with receptors **1** and **2** were described previously [19,22]. To aid comparison, the interaction of anions with receptors **3** and **4** were studied using the same methods and under identical conditions.

The results of ^1H NMR titrations of receptors **3** and **4** with tetrabutylammonium (TBA) chloride in DMSO-d_6 + 0.5% H_2O are presented in Figure 2, together with the results for receptors **1** and **2**. The comparison of chemical shifts of free

receptors **1**-**4** revealed marked influence of the rear substituents X on the position of NH protons. The carbazole NH signal shifts from 9.99 ppm for X=H, through 10.41 ppm for X=Cl and 11.22 ppm for X=CN to 11.49 ppm for X=NO_2. Similar, but smaller downfield shifts (from 9.97 for **1** to 10.39 for **4**) were observed for the amide NHs. It seems therefore, that as the electron withdrawing character of the 3,6-substituents increases, the two NH protons become more and more strongly engaged in hydrogen bonding interactions with the solvent molecules.

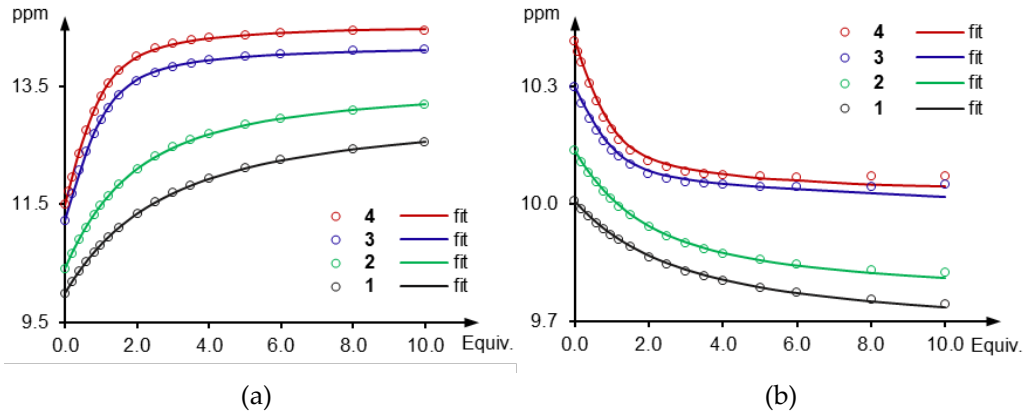

Figure 2. ^{1}H NMR titration curves of the (a) $NH_{carb.}$ and (b) NH_{amide} signals of receptors **1**-**4** (10 mM) for TBACl in DMSO-d_6 + 0.5% H_2O at 298 K. 1:1 model fits are showed as the solid lines.

The addition of TBACl to the solution of each of the four receptors resulted in large downfield shifts of the carbazole NH protons ($\Delta\delta_{max}$ = 2.56, 2.79, 2.89 and 2.98 ppm, respectively) as well as in slight upfield shifts of the amide NHs ($\Delta\delta_{max}$ = -0.27 for **1**, -0.32 for **2**, -0.28 for **3**, -0.37 for **4**). Apparently, the hydrogen bonds formed with the anion by the central carbazole NHs are much stronger than the bonds formed with the two amide side arms. The rather uncommon upfield shifts of the amide protons upon chloride binding by this family of receptors suggest that strong hydrogen bonding interactions with solvent molecules deshields these protons more than the hydrogen bonding with chloride.

These suppositions are supported by the X-ray crystal structures of the chloride complexes of diamides **3** and **4**, in which the carbazole NH-Cl distances are much shorter (2.198 and 2.170 Å, respectively) than the amide NH-Cl distances (2.533 - 2.595 Å), see Figure 3 and Table 1. The asymmetric position of chloride in the cavity of **4** suggests also that while the anion is able to form shorter bonds with amide (2.533 Å), the cavity of the receptor is too wide to allow for the simultaneous formation of two short bonds with this relatively small guest. Very likely therefore, in solution the anion rapidly jumps between two equivalent positions, in which it is closer to either one or another amide arm. Since the observed chemical shifts of the amide protons are averaged over all conformations (fast exchange regime), this hypothesis explains the rather weak effect of chloride binding on the chemical shift of amide protons.

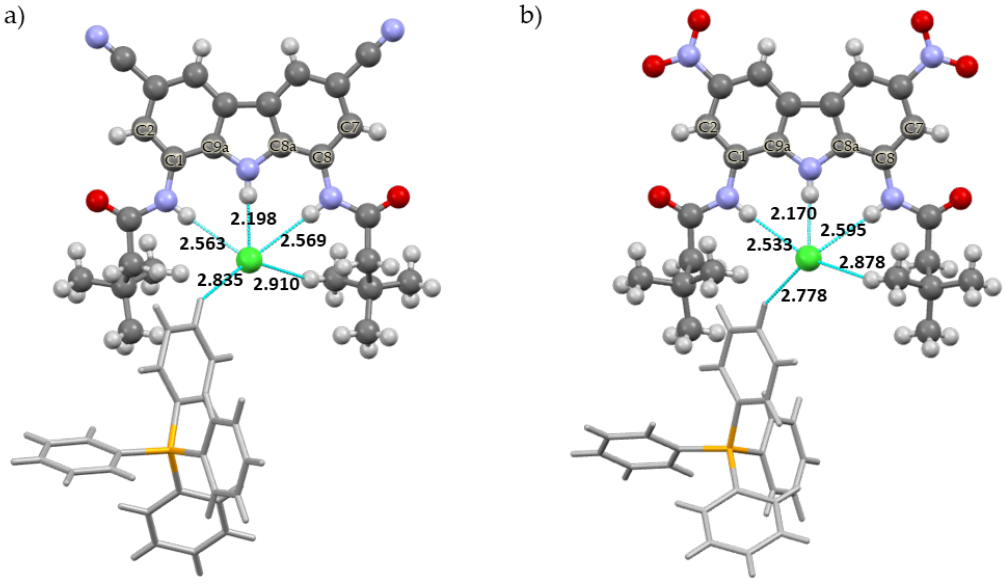

Figure 3. Crystals structures of a) **3**×Cl^- and b) **4**×Cl^-.

Table 1. Hydrogen bonding distances and selected torsion angles in the X-ray crystal structures of chloride complexes of **3** and **4**.

Parameter	Atom	**3**×Cl	**4**×Cl
Bond length, Å	$Cl^-\cdots NH_{carb.}$	2.198	2.170
	$Cl^-\cdots NH_{amide1}$	2.563	2.533
	$Cl^-\cdots NH_{amide2}$	2.569	2.595
	$Cl^-\cdots CH_{t\text{-}Bu}$	2.910	2.878
	$Cl^-\cdots Ph_4P^+$	2.835	2.778
Torsion angle φ, °	C2-C1-N_{amide1}-C_{amide1}	3.80	5.00
	C7-C8-N_{amide2}-C_{amide2}	-5.22	0.38
Torsion angle φ, °	C9a-C1-N_{amide1}-C_{amide1}	-178.32	-176.94
	C9a-C8-N_{amide2}-C_{amide2}	177.43	174.60

Quantitative analysis of the titration curves was performed using web applet BindFit [32]. Excellent fits were obtained using simple 1:1 binding model and the association constants thus obtained are presented in Table 2. As expected, substitution of positions 3 and 6 with strongly electron-withdrawing cyano groups enhances chloride affinity more than 6-fold with respect to the unsubstituted **1** and ca. 2-fold with respect to chlorine substituted **2**. The introduction of even more strongly electron withdrawing nitro groups resulted in further increase in the Cl^- affinity, with binding constant reaching value 7 times higher than for the unsubstituted receptor **1**.

Table 2. Binding constants of receptors **1**-**4** with various anions in DMSO-d_6 + 0.5% H_2O at 298K.

Receptor	K_a Cl^- [a]	K_a $PhCOO^-$	K_a $H_2PO_4^-$	K_a CH_3COO^-
1	48	$10^{3.67}$	$10^{4.01}$	$10^{4.07}$
2	159	$10^{4.47}$	$10^{4.91}$	$10^{4.95}$
3	309	deprotonation	$10^{5.4}$*	n.d.
4	347	deprotonation	deprotonation	n.d.

[a] DMSO-d_6 + 0.5% H_2O;
* - estimated complexation constant, disregarding partial deprotonation.

The binding constants of 1,8-diamidocarbazoles with benzoate and dihydrogen phosphate typically exceed the range which could be reliably determined by NMR titrations. Fortunately, owing to the carbazole chromophore, this class of receptors is perfectly suited for studying anion binding processes using UV-Vis spectroscopy. The addition of oxyanions (as TBA salts) to the solutions of receptors **3** and **4** in DMSO + 0.5% H_2O led to vivid changes in absorbance between 300 and 600 nm (Figure 4).

However, the absence of well-defined isosbestic points and the formation of characteristic peaks at 372 nm (for **3**) and at 515 nm (for **4**), suggest that the observed changes are not only due to anion binding, but also due to proton transfer from the receptors to the basic anions. In case of **3** and $H_2PO_4^-$, the proton transfer becomes significant only after most of the receptor molecules are bound with the anion, which allowed us to estimate anion binding constant from truncated titration curve. The value thus obtained, logK = ca. 5.4, is well in line with the values obtained earlier for **1** and **2** (Table 2) and is also consistent with the expected increase in anion affinity with increasing electron-withdrawing character of the 3,6 substituents. It agrees also with the observed rapid saturation of the complexation-induced changes in the UV-Vis spectra, which occurs after the addition of just 1.6 equivalents of $H_2PO_4^-$ (at 10^{-4} M concentration of **3**). In case of **4**, however, the proton transfer dominates over anion binding, and all attempts to separate the two processes were unsuccessful.

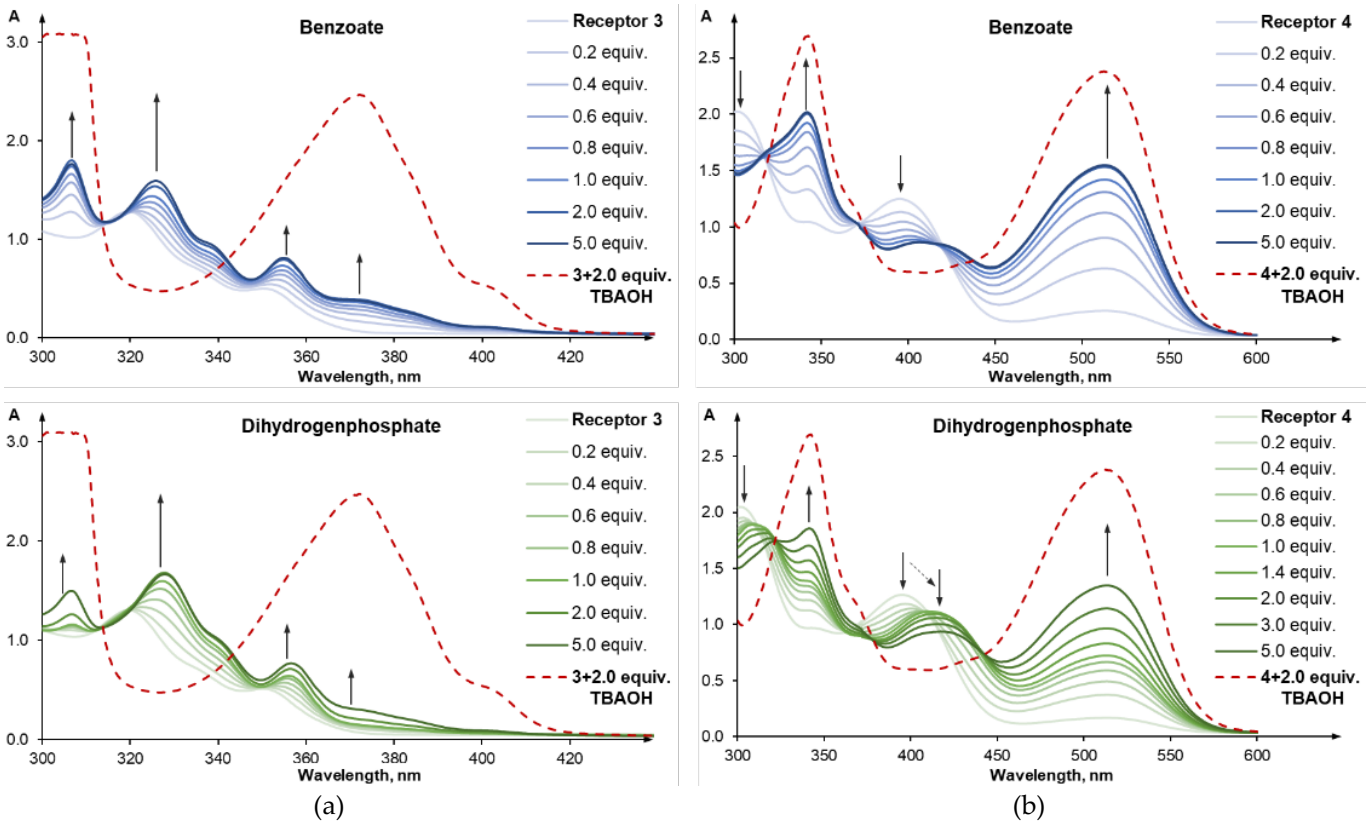

Figure 4. UV-Vis titration of: (a) **3** (10^{-4} M) with TBAPhCOO (up) and $TBAH_2PO_4$ (down); (b) **4** (10^{-4} M) with TBAPhCOO (up) and $TBAH_2PO_4$ (down) in DMSO + 0.5% H_2O at 298 K.

2.3. Self-dissociation studies

Careful analysis of the UV-vis titration data presented above revealed that receptors **3** and **4** are slightly deprotonated even before the addition of any anion (Figure 5). Indeed, further dilution of the receptors beyond the 10^{-4} M concentration used in the titration experiments led to marked increase of the extent of self-ionization, in accord with the Ostwald's dilution law. At 5×10^{-6} M, even the less acidic **3** seems to be completely ionised (Figure 5a). Titration with trifluoromethanesulfonic acid (TfOH) reverses the self-ionization of both receptors (see ESI for **3** and Figure 5b for **4**). It is worth to note that even very small degree of spontaneous dissociation may lead to erroneous conclusions about, *inter alia*, colour, fluorescence, and anion sensing properties of receptors (see, for example, Figure 6). Therefore, we report UV-Vis spectra and photographs of solutions of **3** and **4** in the presence of two equivalents of TfOH (Figure 7).

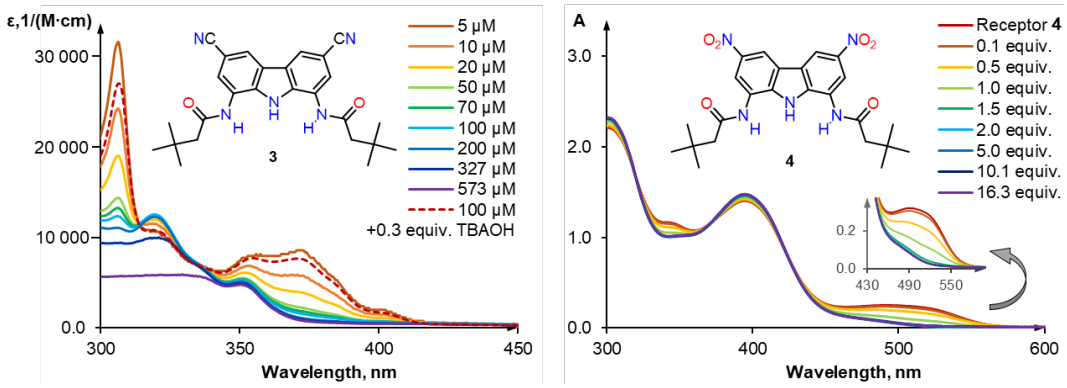

Figure 5. Self-ionization studies. (a) Self-ionization of diluted solutions of **3** in DMSO + 0.5% H_2O at 298 K ($A_{norm.}$=573μM*A/C); (b) Reversal of self-ionization of **4** (10^{-4} M) upon titration with TfOH in DMSO + 0.5% H_2O at 298 K.

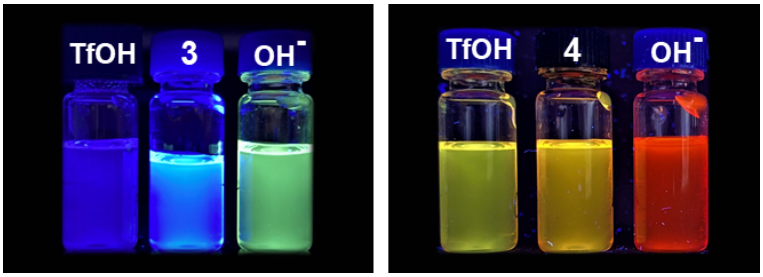

Figure 6. Fluorescence colour change of **3** (left) and **4** (right) at 10^{-4} M in the presence of 2 equivalents of TfOH or 2 equivalents of TBAOH in DMSO + 0.5% H_2O observed under UV lamp (365 nm).

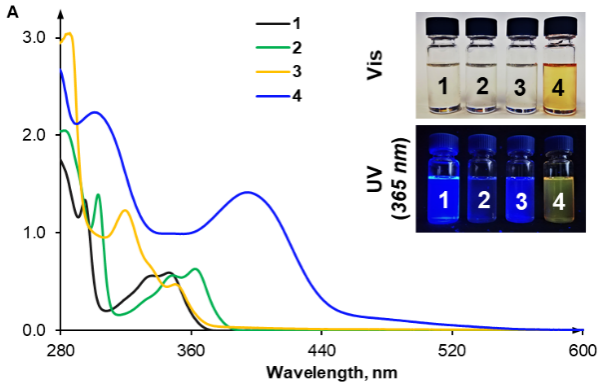

Figure 7. UV-Vis spectra of receptors **1** - **4** (10^{-4} M) in the presence of 2 equiv. of TfOH in DMSO + 0.5% H_2O at 298 K. Inset: the same solutions under visible light and under UV irradiation (365 nm).

2.4. Anion sensing properties of **3** *and* **4**

As shown in Figure 7, the introduction of nitro groups successfully shifted the absorbance spectrum of **4** to the visible region (> 400 nm). Accordingly, both **4** and its solutions are intensely yellow. Similar effect, however, was not observed for cyano groups, and the long wavelength part of the spectrum vanishes even faster for **3** than for **2**.

To investigate the sensory properties of **3** and **4** we added various anions (as their TBA salts) to the solutions of the two receptors in DMSO + 0.5% H_2O (Figure 8). Anions having different shapes, solvation energies and basicity were selected: F^-, Cl^-, Br^-, I^-, NO_3^-, AcO^-, $PhCOO^-$, $H_2PO_4^-$, CN^-, HSO_4^- and SO_4^{2-}.

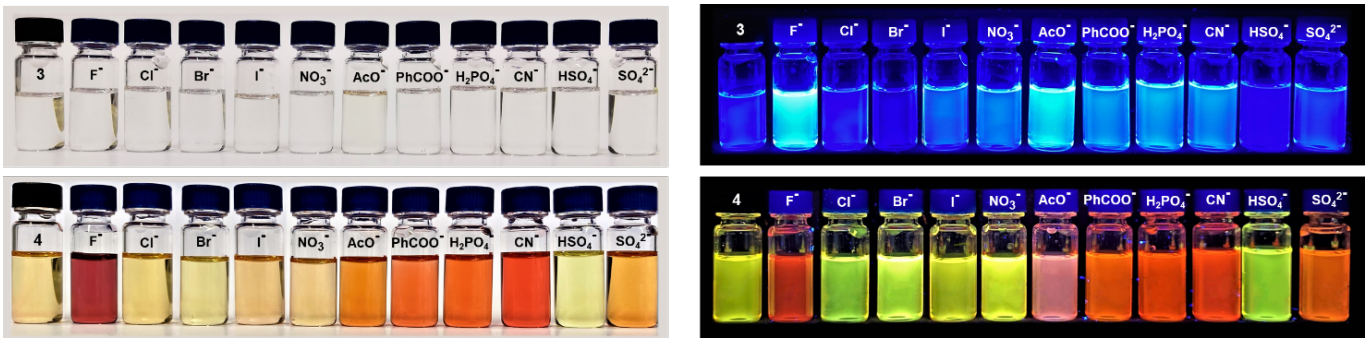

(a) (b)

Figure 8. Colour change of 10^{-4} M solutions of **3** and **4** in the presence of 10 equiv. of various anions (added as their tetrabutylammonium salts) in DMSO + 0.5% H_2O: (a) under ambient light and (b) under UV lamp (365 nm).

No colour change was observed for **3**, in accord with the very weak absorption of **3** and its complexes in the visible region (Figure 4a). Much more significant changes, however, were observed under UV irradiation (λ_{ex} = 365 nm). Significant enhancement in fluorescent emission is clearly visible in all the samples containing the most basic anions: F^-, AcO^-, $PhCOO^-$, $H_2PO_4^-$ and CN^-. This is because the deprotonated **3** is strongly emissive in the visible region. Quenching of fluorescence was observed for HSO_4^-, most likely because this anion acts like Brønsted acid and reverses the spontaneous dissociation of **3**, diminishing the concentration of the highly emissive [**3** - H^+]$^-$.

In contrast, receptor **4** displays a very nice colorimetric response towards F^-, AcO^-, $PhCOO^-$, $H_2PO_4^-$, CN^- and SO_4^{2-}, changing colour from yellow to orange or burgundy (Figure 8a). Almost no change was observed upon addition of Cl^-, Br^-, I^-, NO_3^- and HSO_4^-. Since the colorimetric response is observed only for basic anions and is similar for all of them, it is most likely dominated by the deprotonation of the receptor. As discussed above, both anion binding and receptor deprotonation shift the absorption spectra of **3** and **4** to the right and both processes coexist for $PhCOO^-$ and $H_2PO_4^-$ in wet DMSO. However, in case of the more acidic **4**, proton transfer dominates, and this is further amplified by the fact that the extinction coefficients of $[\mathbf{4} - H^+]^-$ are much higher than of $[\mathbf{4} \times A^-]^-$. As a result, the colorimetric response of **4** is poorly specific, i.e. very similar for all basic anions. Similar behaviour is commonly observed in many hydrogen bonding anion sensors [9].

The above conclusions gain additional support from anion-induced changes in the fluorescence of **4**. Under UV irradiation (365 nm) dramatic changes in emission from yellow-green to orange-red can be seen upon addition of basic anions: F^-, NO_3^-, AcO^-, $PhCOO^-$, $H_2PO_4^-$, CN^- and SO_4^{2-}, whereas little or no change is induced by Cl^-, Br^-, I^-, NO_3^- and HSO_4^-. Again, the weakly basic and weakly binding anions from the latter group cause negligible changes, whereas all the anions from the former group deprotonate **4** to a greater or lesser extent, switching the greenish-yellow fluorescence of the receptor into the orange-red fluorescence of deprotonated receptor. Unlike for **3**, the doubly charged sulfate also deprotonates **4**, in accord with the increased acidity of this receptor.

Unfortunately, more detailed spectrofluorimetric investigations of **3**, **4** and their interaction with anions were hampered by the spontaneous dissociation of the receptors in highly diluted solutions, typically used in fluorescence measurements.

3. Conclusions

In this contribution we describe the synthesis of two novel building blocks for the construction of anion receptors: 1,8-diamino-3,6-dicyanocarbazole **12** and 1,8-diamino-3,6-dinitrocarbazole **16**. Both are interesting not only in the context of anion recognition, but also as high-potential synthons for organic synthesis in general, because they present as many as 5 amino group equivalents on a single carbazole core.

We synthesised also two new 1,8-diamidocarbazole receptors with strongly electron withdrawing 3,6-dicyano and 3,6-dinitro substituents. Both of them display significantly improved anion affinity as compared to the unsubstituted and 3,6-dichloro substituted receptors, but are also much more prone to proton abstraction. Carboxylates, phosphates and sulfate significantly deprotonate these receptors in wet DMSO, what limits their utility in anion recognition. In this way, we have experimentally established the limits of anion affinity enhancement that can be achieved by the substitution of the carbazole platform.

The new 3,6-dinitro substituted receptor **4** acts as colorimetric anion sensor in wet DMSO, producing distinct colour changes upon interaction with basic anions. Unfortunately, however, these changes are mostly due to receptor deprotonation, and therefore lack specificity. In contrast to **4**, the 3,6-dicyano substituted receptor **3** is colourless and produces no significant colour changes upon addition of anions. However, it also undergoes deprotonation by many basic anions, what manifests under UV irradiation as marked enhancement in fluorescence intensity.

Owing to their very high hydrogen bond donating ability combined with relatively high Bronsted acidity, diamidocarbazoles similar to **3** and **4** may find applications in, for example, organocatalysis [33] or in pH-switchable anion transport through lipophilic membranes [34-37]. Research in these directions is ongoing in our laboratories and will be published in due course.

4. Materials and Methods

4.1. General Experimental

4.1.1. Chemicals and Consumables

All solvents and reagents were commercially available and used as received unless otherwise stated. Reagents for this study were purchased from the following vendors:

- Merck-Sigma: *N*,*N*-dimethylacetamide anhydrous (DMA, 99.8%, 271012), 3,3-dimethylbutyryl chloride (*tert*-butylacetyl chloride, 99%, B88802), *N*,*N*-dimethylformamide (DMF, puriss. p.a., ACS reagent, reag. Ph. Eur., ≥99.8% (GC), 33120), dimethyl sulfoxide (DMSO, anhydrous, ≥99.9%, 276855), hydrazine monohydrate ($N_2H_4 \cdot H_2O$, 64-65%, reagent grade, 98%, 207942), iron(II) sulfate heptahydrate ($FeSO_4 \cdot 7H_2O$, ≥99.0%, 215422), methanol (MeOH for HPLC, ≥99.9%, 34860), nitric acid fuming (HNO_3, extra pure, 100%, 1004551000), sodium hydroxide solution (2N NaOH, Titripur, 1091361000), tetrabutylammonium chloride (TBACl, ≥99.0%, 86852), tetrabutylammonium benzoate (TBAPhCOO, ≥99.0%, 86837), tetrabutylammonium phosphate monobasic (TBAH_2PO4, ≥99.0% (T), 86833).

- POCH: acetic acid (AcOH, 99.5-99.9%, pure p.a.-basic, BA8760114), acetic anhydride (Ac_2O, ACS reagent, pure p.a., 693870115), ethyl alcohol anhydrous (EtOH, 99.8% pure p.a., 396480111), nitric acid (HNO_3, 65%, pure p.a., BA9603115), hydrochloric acid (HCl, 35-38%, pure p.a., BA5283115).
- TCI: 1,3,6,8-tetranitrocarbazole (wetted with ca. 40% water, >70.0%, T0159).
- Alfa Aesar: trifluoromethanesulfonic acid (TfOH, anhydrous, 98%).
- Euriso-top: DMSO-d_6 + 0.03%TMS v/v (>99.8% D).

Water was taken from Milli-Q purification system. DMSO/H_2O mixtures were obtained using Milli-Q H_2O and its concentration is expressed as weight-weight percentage.

4.1.2. Instruments and methods

Samples were weighed on Mettler Toledo Excellence XA105DU analytical balance. High-resolution ESI-MS spectra were obtained using a Maldi SYNAPT G2-S HDMS mass spectrometer with direct fusion. Elemental analysis was performed using an automatic UNIcube elemental analyzer. UV-Vis spectra were obtained on Thermo Scientific Evolution 300 UV-Vis spectrophotometer. NMR spectra were recorded using Agilent NMR (^{1}H: 400 MHz, ^{13}C: 100 MHz) spectrometer at ambient temperature in DMSO-d_6. The chemical shifts, δ, are reported in parts per million (ppm) and coupling constants, J, are given in hertz (Hz). The NMR spectra were referenced to the solvent residual signal (^{1}H: δ_{DMSO} = 2.50 ppm, ^{13}C: δ_{DMSO} = 39.50 ppm). Data are reported as follows: chemical shift, multiplicity (s – singlet, bs – broad singlet, d – doublet, t – triplet, dd – doublet of doublets, dt – doublet of triplets, etc.), coupling constant and integration.

4.2. Synthesis

4.2.1. General methods

TLC was carried out on Merck silica gel 60 F_{254} plates. Preparative chromatography was done using a Teledyne Isco CombiFlash system with RediSep Normal-phase Silica Flash Columns. The compositions of eluent mixtures used in chromatographic separations are reported as (v/v) ratios.

4.2.2. Synthesis of the previously reported receptors **1** and **2**

Receptor **1** was obtained in one-step from 1,8-diaminocarbazole [28], as described previously [22]. Receptor **2** was obtained in one-step from 1,8-diamino-3,6-dichlorocarbazole [22], as described previously [19].

4.2.3. Synthesis of receptor **3**

Receptor **3** was obtained in a three-steps synthesis from the previously described 3,6-dicyjanocarbazole **10** [29].

Synthesis of 3,6-dicyano-1,8-dinitrocarbazole **11**

To a 50 ml round-bottom two-neck flask equipped with a magnetic stirrer 3,6-dicyanocarbazole (0.652 g, 3.00 mmol), acetic anhydride (10 ml, 0.11 mol) and acetic acid (13 ml, 0.23 mol) were added. The flask was equipped with a reflux condenser connected to a check-valve bubbler and through the side neck of the flask 100% nitric acid (0.79 ml, 19 mmol) was added drop-by-drop using Pasteur pipette. The neck was tightly closed with a glass stopper and the mixture was heated with stirring to 110°C (measured in oil bath). After 50 minutes (from the beginning of the heating), the reaction mixture was cooled down for 10 minutes at room temperature and another portion of 100% nitric acid (0.79 ml, 19 mmol) was added. The mixture was heated to 110°C again and this procedure was repeated four times: 3.16 ml (76 mmol) of nitric acid were added in total. The addition of the fifth portion of 100% nitric acid (0.79 ml, 19 mmol) was preceded by the addition of acetic anhydride (2 ml, 21 mmol). This procedure was repeated five times: 10 ml (105 mmol) of acetic anhydride and 3.95 ml (95 mmol) of nitric acid were added in total. After the eighth addition of HNO_3/HNO_3+Ac_2O the progress of the reaction was checked by ^{1}H NMR and additional portions of HNO_3+Ac_2O were added until the signal from 3,6-dicyano-1-mononitrocarbazole disappeared. After cooling the reaction mixture to RT, 50 ml of deionized water were added. The precipitate was filtered off and washed with water (2 × 15 ml), MeOH (2 × 5 ml) and diethyl ether (2 × 5 ml). Vacuum drying yielded pure product as a yellow powder (0.609 g, 66%).

^{1}H NMR (400 MHz, DMSO-d_6) δ_{DMSO}: 11.79 (s, 1H, $NH_{carb.}$), 9.30 (d, *J* 1.43, 2H, CH4/5 or CH2/7), 8.98 (d, *J* 1.41, 2H, CH4/5 or CH2/7); ^{13}C NMR (101 MHz, DMSO-d_6) δ_{DMSO}: 135.23, 133.35; 133.07, 127.92, 125.26, 117.49, 104.32; HR MS (ESI): *m*/*z* calcd. for $C_{14}H_4N_5O_4$ $[M-H]^-$: 306.0269 found: 306.0263.

Synthesis of 1,8-diamino-3,6-dicyanocarbazole

To a 50 ml round-bottom two-neck flask equipped with a magnetic stirrer, 3,6-dicyano-1,8-dinitrocarbazole (0.614 g, 2.00 mmol) and anhydrous EtOH (30 ml) were added. The flask was equipped with a reflux condenser connected to a check-valve bubbler, the side neck was sealed with a septum and argon was bubbled through the mixture for 10 minutes with slow stirring. After this time, $FeSO_4 \cdot 7H_2O$ (37 mg, 0.13 mmol) was added and argon was bubbled through the mixture for additional 15 min. Then, in the flow of argon, 98% hydrazine monohydrate $NH_2NH_2 \cdot H_2O$ (3.90 ml, 80 mmol) was added dropwise. The mixture was heated to reflux and stirred for 48h. After cooling to RT, the precipitate was filtered off and suspended in dimethylformamide (ca. 7 ml). The product dissolved in DMF and was separated from insoluble impurities by filtration. Next, methanol (60 ml) was added to the filtrate and precipitated impurities were filtered off again using G4 sintered glass filter. Finally, deionized water (40 ml) with a few droplets of hydrazine monohydrate (to protect the product from air oxidation) was added to the filtrate in order to precipitate the desired product. The suspension was boiled for 10 minutes, cooled down to RT and put into a refrigerator for 24h. The product was filtered off and washed with water (3 × 3 ml). Vacuum drying yielded product which was sufficiently pure for subsequent reaction (brown powder, 0.096 g, 20%).

^{1}H NMR (400 MHz, DMSO-d_6) δ_{DMSO}: 11.46 (s, 1H, NH_{carb}), 7.94 (d, *J* 1.36, 2H, CH4/5 or CH2/7), 6.95 (d, *J* 1.47, 2H, CH4/5 or CH2/7), 5.58 (s, 4H, NH_2); ^{13}C NMR (101 MHz, DMSO-d_6) δ_{DMSO}: 135.23, 133.35, 133.07, 127.92, 125.26, 117.49, 104.32; HR MS (ESI): *m*/*z* calcd. for $C_{14}H_8N_5$ $[M-H]^-$: 246.0785 found: 246.0780.

Synthesis of receptor **3**

A 5 ml round-bottom flask was dried with a heat gun (set to ca. 500°C) for 10 minutes, and then cooled down to RT in a desiccator. To the flask, 1,8-diamino-3,6-dicyanocarbazole (0.050 g, 0.20 mmol) and a magnetic stirrer were added. The neck of the flask was sealed with a septum and the flask was filled with argon by three pump-thaw cycles. Anhydrous dimethylacetamide (3 ml) was added via a syringe, followed by the addition of 3,3-dimethylbutyryl chloride (0.090 ml, 0.64 mmol). The reaction mixture was stirred at RT for 20h. After this time, the reaction mixture was poured into deionized water (25 ml). The precipitate was filtered off and washed with water (3 × 3 ml), 5% MeOH/DCM (2 × 3 ml) and ACN (3 × 3 ml). The crude product was purified by column chromatography on 30 g of silica gel using 3% MeOH/DCM as an eluent. The progress of the chromatographic separation was monitored with TLC using 60% EtOAc/Hexane as an eluent. Fractions containing pure product were combined and evaporated to yield 0.032 g (36%) of the desired product as brown solid.

^{1}H NMR (400 MHz, DMSO-d_6) δ_{DMSO}: 11.23 (s, 1H, NH_{carb}), 10.26 (s, 2H, NH_{amide}), 8.54 (d, *J* 1.3, 2H, CH2/7 or CH4/5), 7.97 (d, *J* 1.12, 2H, CH2/7 or CH4/5), 2.38 (s, 4H, CH_2) 1.10 (s, 18H, *t*-Bu); ^{13}C NMR (101 MHz, DMSO-d_6) δ_{DMSO}: 170.77, 134.56, 124.36, 123.71, 122.45, 122.15, 119.60, 102.26, 49.03, 30.98, 29.64; HR MS (ESI): *m*/*z* calcd. for $C_{26}H_{29}N_5O_2Na$ $[M+Na]^+$: 466.2213, found: 466.2219.

4.2.4. Synthesis of Receptor **4**

Receptor **4** was obtained in two steps from commercially available 1,3,6,8-tetranitrocarbazole.

Synthesis of 1,8-diamino-3,6-dinitrocarbazole

Prior to the synthesis, the commercially available 1,3,6,8-tetranitrocarbazole (wetted with ca. 40% water) was dried in a vacuum desiccator over KOH to a constant mass.

To a 25 ml round-bottom two-neck flask equipped with a magnetic stirrer, 1,3,6,8-tetranitrocarbazole (0.200 g, 0.58 mmol) and anhydrous EtOH (10 ml) were added. The flask was equipped with a reflux condenser connected to a check-valve bubbler, the side neck was sealed with a septum and argon was bubbled through the mixture for 10 minutes with slow stirring. After this time $FeSO_4 \cdot 7H_2O$ (10 mg, 0.036 mmol) was added. Argon was bubbled through the mixture for additional 15 min. Then, in the flow of argon, hydrazine monohydrate (98% $NH_2NH_2 \cdot H_2O$, 1.20 ml, 25 mmol) was added dropwise. The mixture was heated to reflux and stirred for 20h. After cooling to RT, the precipitate was filtered off, sonicated with MeOH for 10 min and filtered off once again. Vacuum drying yielded product as dark brown powder (0.130 g, 78%). The product was used for the subsequent reaction without any additional purification.

^{1}H NMR (400 MHz, DMSO-d_6) δ_{DMSO}: 11.71 (s, 1H, NH_{carb}), 8.58 (s, 2H, CH4/5 or CH2/7), 7.62 (s, 2H, CH4/5 or CH2/7), 5.76 (s, 4H, NH_2); ^{13}C NMR (101 MHz, DMSO-d_6) δ_{DMSO}: 142.07, 134.70, 133.05, 122.68, 106.74, 103.80; HR MS (ESI): *m*/*z* calcd. for $C_{12}H_8N_5O_4$ $[M-H]^-$: 286.0576, found: 286.0565.

Synthesis of receptor **4**

A 25 ml round-bottom flask was dried with a heat gun (set to ca. 500°C) for 10 minutes, and then cooled down to RT in a desiccator. To the flask, 1,8-diamino-3,6-dinitrocarbazole (0.190 g, 1.00 mmol) was added, followed by a magnetic stirrer. The neck of the flask was sealed with septum and the flask was filled with argon by three pump-thaw cycles. Anhydrous dimethylacetamide (10 ml) was added *via* a syringe followed by the addition of 3,3-dimethylbutyryl chloride (0.420 ml, 3.00 mmol). The reaction was stirred at RT for 20h. After this time, the reaction mixture was poured into deionized water (100 ml), cooled down in a refrigerator for 20 min and the participate was filtered off and washed with water (3 × 3 ml) and MeOH (2 × 3 ml). Slightly contaminated product was suspended in acetone (80 ml), sonicated for 10 min and filtered off. Vacuum drying yielded pure product as yellow powder (0.280 g, 58 %).

^{1}H NMR (400 MHz, DMSO-d_6) δ_{DMSO}: 11.49 (s, 1H, NH_{carb}), 10.38 (s, 2H, NH_{amide}), 9.28 (d, *J* 2.2, 2H, CH4/5), 8.55 (d, *J* 2.1, 2H, CH2/7), 2.40 (s, 4H, CH_2) 1.11 (s, 18H, *t*-Bu); ^{13}C NMR (101 MHz, DMSO-d_6) δ_{DMSO}: 170.90, 141.17, 136.07, 123.85, 123.77, 114.54, 114.53, 49.04, 30.99, 29.62; HR MS (ESI): *m/z* calcd. for $C_{24}H_{28}N_5O_6Na$ [M-H]$^-$: 482.2040, found: 482.2038; Elemental Analysis calcd. for $C_{24}H_{29}N_5O_6$: C, 59.62; H, 6.05; N, 14.48; found: C, 59.28; H, 6.07; N, 14.21.

4.3. Binding Studies

4.3.1. Typical procedure for ^{1}H NMR titration

All the reagents were weighted separately on an analytical balance (readability 0.01 mg) in screw-capped vials sealed with Teflon-covered septa. DMSO-d_6 + 0.5% H_2O (w/w) mixture was prepared and used as a solvent. All the solvents/solutions manipulations were done using gas-tight Hamilton glass syringes. Titrant was prepared by dissolving TBACl in the solution of the receptor, in order to avoid dilution of the receptor during titration. To a solution of host (600 μl, 0.01 M) in a septum-sealed screw-capped NMR tube sealed with Teflon-covered septum, appropriate aliquots of titrant (up to 10 equiv., 0.3 M, dissolved in the solution of host to avoid dilution) were added with a 25 μl gas-tight microsyringe. ^{1}H NMR spectrum was recorded after each addition of the salt, and the temperature inside the NMR probe was kept constant at 25 °C. Association constants were calculated from changes in the chemical shifts of the most affected protons of the ligands, as indicated in each case below.

4.3.2. Typical procedure for UV-Vis titration

All the reagents were weighted separately on an analytical balance (readability 0.01 mg) in screw-capped vials sealed with Teflon-covered septa. DMSO-d_6 + 0.5% H_2O (w/w) mixture was prepared and used as a solvent. All the solvents/solutions manipulations were done using gas-tight Hamilton glass syringes. Titrants were prepared by dissolving an appropriate amount of TBA salt in the solution of the receptor, in order to avoid dilution of the receptor during titration.

Typically, to a solution of host (3 ml, 10^{-4} M) in a septum-sealed screw-cap precision cell made of SUPRASIL Quartz (light path: 10 mm) appropriate aliquots of titrant (7.5×10^{-3} M, dissolved in the solution of host to avoid dilution) were added with a 25 μl gas-tight microsyringe. The absorption spectra were recorded between 280 and 600 nm after each addition of the salt at 25 °C. Association constants were calculated from changes in absorbance at fixed wavelengths, as detailed below.

4.3.3. Data fitting

The association constants were determined from NH_{amide} and $NH_{carb.}$ resonances using global fitting analysis. This was performed using the BindFit web applet and the 1:1 binding model (Nelder-Mead method, 'Subtract initial values' = ON). In all cases, the 1:1 model gave very good fit to the data, as well as reasonable values of binding constants.

The UV-Vis titration data were fitted with HypSpec software. Association constants and molar absorption coefficients of complexes were set as free parameters for fitting. Logarithms of association constants were averaged using arithmetic mean from at least two separate experiments.

4.4. Self-dissociation studies

4.4.1. Typical procedure for trifluoromethanesulfonic acid titration

All the reagents were weighted separately on an analytical balance (readability 0.01 mg) in screw-capped vials sealed with Teflon-covered septa. DMSO-d_6 + 0.5% H_2O (w/w) mixture was prepared and used as a solvent. All the solvents/solutions manipulations were done using gas-tight Hamilton glass syringes. Titrant was prepared by

dissolving trifluoromethanesulfonic acid TfOH in the solution of the receptor (in order to avoid dilution of the receptor during titration).

Typical, to a solution of host (3 ml, 10^{-4} M) in a septum-sealed screw-cap precision cell made of SUPRASIL Quartz (light path: 10 mm) appropriate aliquots of titrant (7.5×10^{-3} M, dissolved in the solution of host to avoid dilution) were added with a 25 μl gas-tight microsyringe. The absorption spectra were recorded between 280 and 600 nm after each addition of the acid at 25 °C.

4.5. Single crystal X-ray diffraction analysis

Good quality single crystals for X-ray structural investigations were obtained by slow diffusion of pentane into dichloroethane solutions containing receptors **3** or **4** and Ph_4PCl. Diffraction data were collected on the Agilent Technologies SuperNova Dual Source with the MoKα radiation (λ = 0.71073 Å). The lattice parameters were obtained by least-squares fit to the optimized setting angles of the reflections collected by using the CrysAlis CCD software [38]. Data were reduced using the CrysAlis RED program [38]. The gaussian numerical absorption correction using a multi-faceted crystal model implemented in SCALE3 ABSPACK scaling algorithm, was applied [38]. Using Olex2 [39], the structure was solved with the ShelXT [40] structure solution program using Intrinsic Phasing and refined with the ShelXl [41] refinement package using Least Squares minimisation. All H-atoms were positioned geometrically. The crystallographic data are summarized in Table S1. The values of bond lengths and valence angles are given in Tables S2–S3.

Supplementary Materials: The following are available online: Figure S1: ^{1}H NMR spectrum of 3,6-dicyjano-1,8-dinitrocarbazole in DMSO-d_6; Figure S2: ^{13}C NMR spectrum of 3,6-dicyjano-1,8-dinitrocarbazole in DMSO-d_6; Figure S3: ^{1}H NMR spectrum of 1,8-diamino-3,6-dicyjanocarbazole in DMSO-d_6; Figure S4: ^{13}C NMR spectrum of 1,8-diamino-3,6-dicyjanocarbazole in DMSO-d_6; Figure S5: ^{1}H NMR spectrum of **3** in DMSO-d_6; Figure S6: ^{13}C NMR spectrum of **3** in DMSO-d_6; Figure S7: ^{1}H NMR spectrum of 1,8-diamino-3,6-dinitrocarbazole in DMSO-d_6; Figure S8: ^{13}C NMR spectrum of 1,8-diamino-3,6-dinitrocarbazole in DMSO-d_6; Figure S9: ^{1}H NMR spectrum of **4** in DMSO-d_6; Figure S10: ^{13}C NMR spectrum of **4** in DMSO-d_6; Figure S11: ^{1}H ROESY spectrum of **4** in DMSO-d_6; Scheme S1: Amide groups conformations in **4**; ^{1}H NMR spectra of titration with TBACl in DMSO-d_6 + 0.5% H_2O, raw data, titration curves obtained from chemical shifts of $NH_{carb.}$ and NH_{amide} protons; UV-Vis spectra from titrations with TBA salts in DMSO-d_6 + 0.5% H_2O, raw data; UV-Vis spectra of self-dissociation reversing titration with TfOH in DMSO-d_6 + 0.5%H_2O, titration curves; crystallographic data and refinement details. Crystallographic data for the structures in this paper have been deposited with the Cambridge Crystallographic Data Centre as supplementary publication number CCDC 2074344 and 2074345. Copies of the data can be obtained, free of charge, on application to CCDC [e- mail: deposit@ccdc.cam.ac.uk, website: www.ccdc.cam.ac.uk].

Funding: This work was supported by the National Science Centre, Poland (OPUS grant 2018/31/B/ST5/02085 to M.J.C.) This study was carried out at the Biological and Chemical Research Centre, University of Warsaw, established within a project co-financed by the European Union through the European Regional Development Fund under the Operational Programme Innovative Economy 2007–2013.

Acknowledgments: We thank dr Szymon Sutuła from the Core Facility for Crystallography and Biophysics for the excellent crystallographic service he provides.

References

1. Busschaert, N.; Caltagirone, C.; Rossom, W. Van.; Gale, P. A. Applications of Supramolecular Anion Recognition. *Chem. Rev.*, **2015**, *115*, 8038-8155. DOI: 10.1021/acs.chemrev.5b00099.

2. Gunnlaugsson, T.; Kruger, P. E.; Jensen, P.; Tierney, J.; Ali, H. D. P.; Hussey, G. M. Colorimetric "Naked Eye" Sensing of Anions in Aqueous Solution. *J. Org. Chem.*, **2005**, *70(26),* 10875-8. DOI: 10.1021/jo0520487.

3. Hiscock, J. R.; Caltagirone, C.; Light, M. E.; Hursthouse, M. B.; Gale, P. A. Fluorescent carbazolylurea anion receptors. *Org. Biomol. Chem.*, **2009**, *7*, 1781-1783. DOI: 10.1039/B900178F.

4. Zapata, F.; Caballero, A.; White, N. G.; Claridge, T. D. W.; Costa, P. J.; Félix, V.; Beer, P. D. Fluorescent Charge-Assisted Halogen-Bonding Macrocyclic Halo-Imidazolium Receptors for Anion Recognition and Sensing in Aqueous Media. *J. Am. Chem. Soc.*, **2012**, *134*, 28, 11533-11541. DOI: 10.1021/ja302213r.

5. Al-Sayah, M. H.; Abdalla, A. M.; Shehab, M. K. A dansyl-based optical probe for detection of singly and doubly charged anions. *Supramol. Chemistry*, **2016**, *28*, 224-230, DOI: 10.1080/10610278.2015.1091456.

6. Casula, A.; Bazzicalupi, C.; Bettoschi, A.; Cadoni, E.; Coles, S. J.; Horton, P. N.; Isaia, F.; Lippolis, V.; Mapp, L. K.; Marini, G. M.; Montis, R.; Scorciapino, M. A., Caltagirone, C. Fluorescent asymmetric bis-ureas for pyrophosphate recognition in pure water. *Dalton Trans*., **2016**, *45*, 3078-3085. DOI: 10.1039/c5dt04497a.

7. Navarro-García, E.; Velasco, M. D.; Zapata, F.; Bauzá, A.; Frontera, A.; Ramírez de Arellano, C.; Caballero, A. Exploiting 1,4-naphthoquinone and 3-iodo-1,4-naphthoquinone motifs as anion binding sites by hydrogen or halogen-bonding interactions. *Dalton Trans*., **2019**, *48*, 11813-11821. DOI: 10.1039/C9DT02012H.

8. Gale P. A.; Caltagirone, C. Fluorescent and colorimetric sensors for anionic species. *Coord. Chem. Rev*., **2018**, *354*, 2-27. DOI: 10.1016/j.ccr.2017.05.003.

9. McNaughton, D. A.; Fares, M.; Picci, G.; Gale, P. A.; Caltagirone, C. Advances in fluorescent and colorimetric sensors for anionic species. *Coordination Chemistry Reviews,* **2021**, *427*, 213573. DOI: 10.1016/j.ccr.2020.213573.

10. Chmielewski, M. J.; Charon, M.; Jurczak, J. 1,8-Diamino-3,6-dichlorocarbazole: A Promising Building Block for Anion Receptors. *Org. Lett*. **2004**, *6*, 3501-3504. DOI: 10.1021/ol048661e.

11. Piątek, P.; Lynch, V. M.; Sessler, L. J.; Calix[4]pyrrole[2]carbazole: A New Kind of Expanded Calixpyrrole. *J. Am. Chem. Soc*., **2004**, *126*, 49, 16073-16076. DOI: 10.1021/ja045218q.

12. Thangadurai, T. D.; Singh, N. J.; Hwang, I.-C.; Lee,J. W.; Chandran, R. P.; Kim. K. S. 2-Dimensional Analytic Approach for Anion Differentiation with Chromofluorogenic Receptors. *J. Org. Chem*. **2007**, *72*, 14, 5461-5464. DOI: 10.1021/jo070791o.

13. Gross, D. E.; Vinay Mikkilineni, Vincent M. Lynch, and Jonathan L. Sessler, Bis-amidopyrrolyl Receptors Based on Anthracene and Carbazole. *Supramol Chem*., **2010**, *22*, 135-141. DOI: 10.1080/10610270903304434.

14. Hiscock, J. R.; Gale, P. A.; Caltagirone , C.; Hursthouse, M. B.; Light, M. E. Fluorescent carbazolylurea- and carbazolylthiourea-based anion receptors and sensors. *Supramol. Chem.*, **2010**, *22*, 647-652. DOI:10.1080/10610271003637087

15. Ahmed, N.; Geronimo, I.; Hwang, I.-C.; Singh, J.; Kim. K. S. *cyclo*-Bis(urea-3,6-dichlorocarbazole) as a Chromogenic and Fluorogenic Receptor for Anions and a Selective Sensor of Zinc and Copper Cations. *Chem. Eur. J.* **2011**, *17*, 8542-8548. DOI: 10.1002/chem.201100243.

16. Yang, Y.; Xue, M.; Marshall, L. J.; de Mendoza, J. Hydrogen-Bonded Cyclic Tetramers Based on Ureidopyrimidinones Attached to a 3,6-Carbazolyl Spacer. *Org. Lett*. **2011**, *13*, 12, 3186-3189. DOI: 10.1021/ol200946b.

17. Fuentes de Arriba, A. L.;Turiel, M. G.; Simón, L.; Sanz, F.; Boyero, J. F.; Muñiz, F. M.; Morána, J. R.; Alcázar, V. Sulfonamide carbazole receptors for anion recognition. *Org. Biomol. Chem.,* **2011**, *9*, 8321-8327. DOI: 10.1039/C1OB06126G.

18. Sanchez, G.; Espinosa, A.; Curiel, D.; Tarraga, A.; Molina, P. Bis(carbazolyl)ureas as Selective Receptors for the Recognition of Hydrogenpyrophosphate in Aqueous Media. *J. Org. Chem*., **2013**, *78*, *19*, 9725-9737. DOI: 10.1021/jo401430d.

19. Bąk, K. M.; Chmielewski, M. J. Sulfate templated assembly of neutral receptors in aqueous DMSO – orthogonal versus biplane structures. *Chem. Commun*. **2014**, *50*, 1305-1308. DOI: 10.1039/C3CC48463G.

20. Bąk, K. M.; Masłowska, K.; Chmielewski, M. J. Selective turn-on fluorescence sensing of sulfate in aqueous–organic mixtures by an uncharged bis(diamidocarbazole) receptor. *Org. Biomol. Chem.,* **2017**, *15*, 5968-5975. DOI: 10.1039/C7OB01358B.

21. Martin, K.; Nõges, J.; Haav, K.; Kadam, S. A.; Pung, A.; Leito, I. Exploring Selectivity of 22 Acyclic Urea-, Carbazole- and Indolocarbazole- Based Receptors towards 11 Monocarboxylates. *Eur. J. Org. Chem.* **2017**, *35*, 5231-5237. DOI: 10.1002/ejoc.201700931.

22. Bąk, K. M.; Chabuda, K.; Montes, H.; Quesada, R.; Chmielewski, M. J. 1,8-Diamidocarbazoles: an easily tuneable family of fluorescent anion sensors and transporters. *Org. Biomol. Chem*. **2018**, *16*, 5188-5196. DOI: 10.1039/C8OB01031E.

23. Rüütel, A.; Yrjänä, V.; Kadam, S. A.; Saar, I.; Ilisson, M.; Darnell, A.; Haav, K.; Haljasorg, T.; Toom, L.; Bobacka, J.; Leito, I. Design, synthesis and application of carbazole macrocycles in anion sensors. *Beilstein J Org Chem*., **2020**, *16*, 1901-1914. DOI: 10.3762/bjoc.16.157.

24. Yrjänä, V.; Saar, I.; Ilisson, M.; Kadam, S. A.; Leito, I.; Bobacka, J. Potentiometric Carboxylate Sensors Based on Carbazole-Derived Acyclic and Macrocyclic Ionophores. *Chemosensors*, **2021**, *9*, 4. DOI: 10.3390/chemosensors9010004.

25. Bąk, K. M.; Kolck, B. van.; Maslowska-Jarzyna, K.; Papadopoulou, P.; Kros, A.; Chmielewski, M. J. Oxyanion transport across lipid bilayers: direct measurements in large and giant unilamellar vesicles. *Chem. Commun*. **2020**, *56*, 4910-4913. DOI: 10.1039/C9CC09888G.

26. Pomorski, R.; García-Valverde, M.; Quesada, R.; Chmielewski, M. J. Transmembrane anion transport promoted by thioamides. *RSC Advances*, accepted.

27. Muzık, F.; Allan, Z.; Poskocil, J. Derivate des Carbazols IV. Herstellung von 3,6-Dichlor-1,8-diaminocarbazol. *Collect. Czech. Chem. Commun*., **1958**, *23*, 770-772. DOI: 10.1135/cccc19580770.

28. Fedorczyk, A.; Pomorski, R.; Chmielewski, M. J.; Ratajczak, J.; Kaszkur, Z.; Skompska, M. Bimetallic Au@Pt nanoparticles dispersed in conducting polymer—A catalyst of enhanced activity towards formic acid electrooxidation. *Electrochim. Acta,* **2017**, *246*, 1029-1041. DOI: 10.1016/j.electacta.2017.06.

29. Weselinski, L. J.; Luebke, R.; Eddaoudi, M. A Convenient Preparation of 9H-Carbazole-3,6-dicarbonitrile and 9H-Carbazole-3,6-dicarboxylic Acid. *Synthesis,* **2014**, *46*, 596-599. DOI: 10.1055/s-0033-1340557.

30. Andreozzi, R.; Marotta, R.; Sanchirico, R. Thermal decomposition of acetic anhydride–nitric acid mixtures. *Journal of Hazardous Materials*, **2002**, *90*, 111-121. DOI: 10.1016/S0304-3894(01)00356-9.

31. Sharma, U.; Verma, P. K.; Kumar, N.; Kumar, V.; Bala, M.; Singh, B. Phosphane-Free Green Protocol for Selective Nitro Reduction with an Iron-Based Catalyst. *Chem. Eur. J.,* **2011**, *17*, 5903-5907. DOI: 10.1002/chem.201003621.

32. Bindfit-Fit Data to 1:1 Host-Guest Equilibria. Available online: http://supramolecular.org (accessed on 16 March 2021).

33. Zhanga, Z.; Schreiner, P. R. (Thio)urea organocatalysis—What can be learnt from anion recognition? *Chem. Soc. Rev*., **2009**, *38*, 1187-1198. DOI: 10.1039/B801793J.

34. Elmes; R. B. P.; Busschaert, N.; Czech, D. D.; Gale, P. A.; Jolliffe, K. A. pH switchable anion transport by an oxothiosquaramide. *Chem. Commun*., **2015**, *51*, 10107-10110. DOI: 10.1039/c5cc03625a.

35. Saha, A.; Akhtar, N.; Kumar, V.; Kumar, S.; Srivastava, H. K.; Kumarb, S.; Manna, D. pH-Regulated anion transport activities of bis (iminourea) derivatives across the cell and vesicle membrane. *Org. Biomol. Chem*., **2019**, *17*, 5779-5788. DOI: 10.1039/c9ob00650h.

36. Howe, E. N. W.; Busschaert, N.; Wu, X.; Berry, S. N.; Ho, J.; Light, M. E.; Czech, D. D.; Klein, H. A.; Kitchen, J. A.; Gale, P. A. pH-Regulated Nonelectrogenic Anion Transport by Phenylthiosemicarbazones. *J. Am. Chem. Soc*., **2016**, *138*, 8301-8308. DOI: 10.1021/jacs.6b04656.

37. Busschaert, N.; Elmes, R. B. P.; Czech, D. D.; Wu, X.; Kirby, I. L.; Peck, E. M.; Hendzel, K. D.; Shaw, S. K.; Chan, B.; Smith, B. D.; Jolliffe K. A.; Gale, P. A. Thiosquaramides: pH switchable anion transporters. *Chem. Sci*., **2014**, *5*, 3617-3626. DOI: 10.1039/c4sc01629g.

38. *CrysAlis CCD and CrysAlis RE*D; Oxford Diffraction Ltd: Yarnton, **2008**.

39. Dolomanov, O. V.; Bourhis, L .J.; Gildea, R. J.; Howard, J.A.K.; Puschmann, H. *J. Appl. Cryst*. **2009**, *42*, 339-341.

40. Sheldrick, G. M. *Acta Cryst. A71*, **2015**, 3-8.

41. Sheldrick, G. M. *Acta Cryst. C71*, **2015**, 3-8.

Supporting Information

Carbazole-based colorimetric anion sensors

Krystyna Maslowska-Jarzyna, Maria L. Korczak, Jakub Wagner and Michał J. Chmielewski*

Faculty of Chemistry, Biological and Chemical Research Centre, University of Warsaw

Żwirki i Wigury 101, 02-089 Warszawa, Poland

E-mail: mchmielewski@chem.uw.edu.pl

Contents

1 NMR spectra

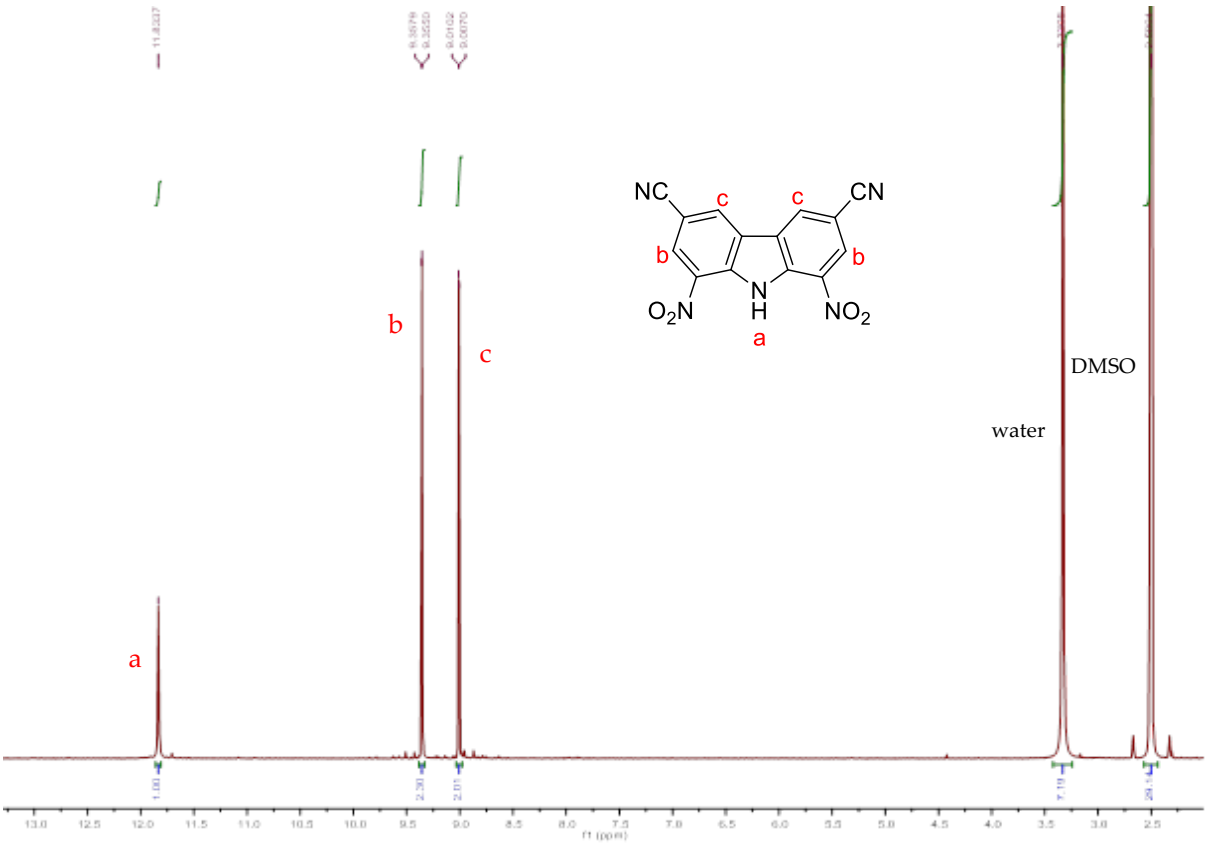

Figure S1. ^{1}H NMR spectrum of 3,6-dicyjano-1,8-dinitrocarbazole in DMSO-d_6.

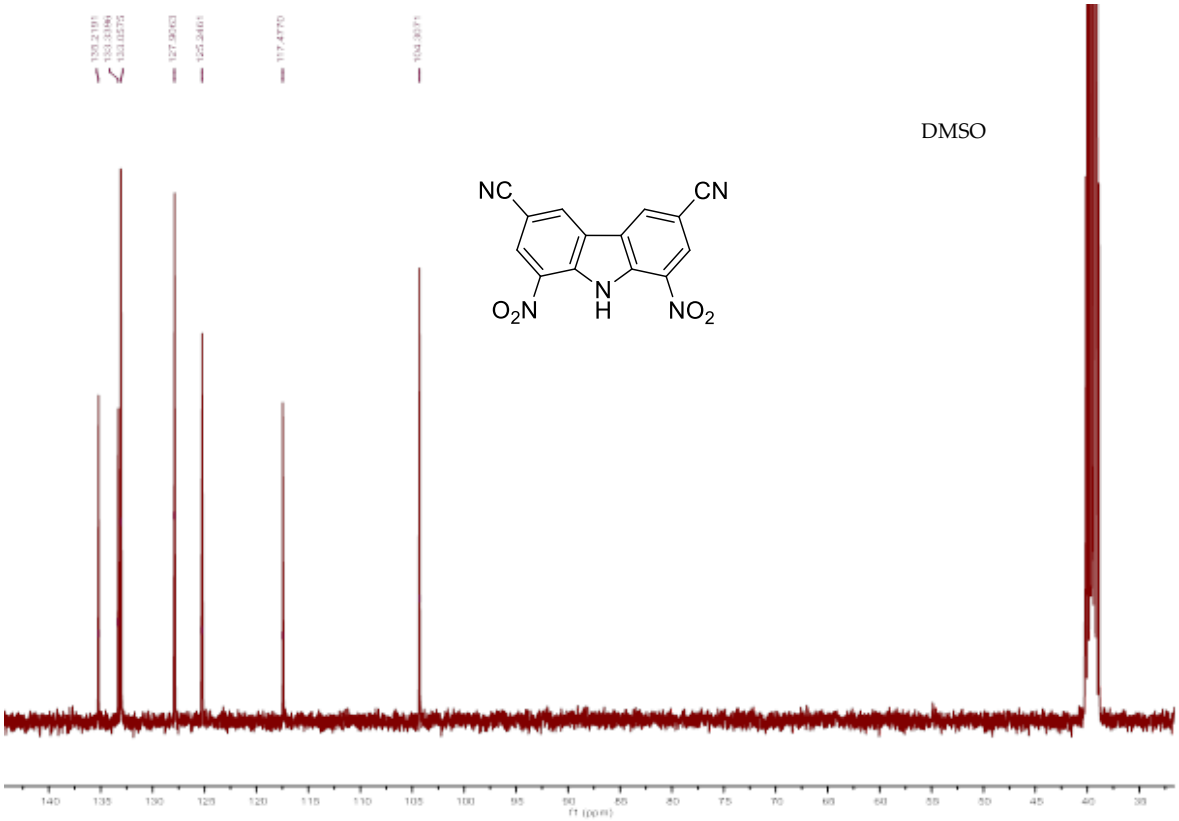

Figure S2. ^{13}C NMR spectrum of 3,6-dicyjano-1,8-dinitrocarbazole in DMSO-d_6.

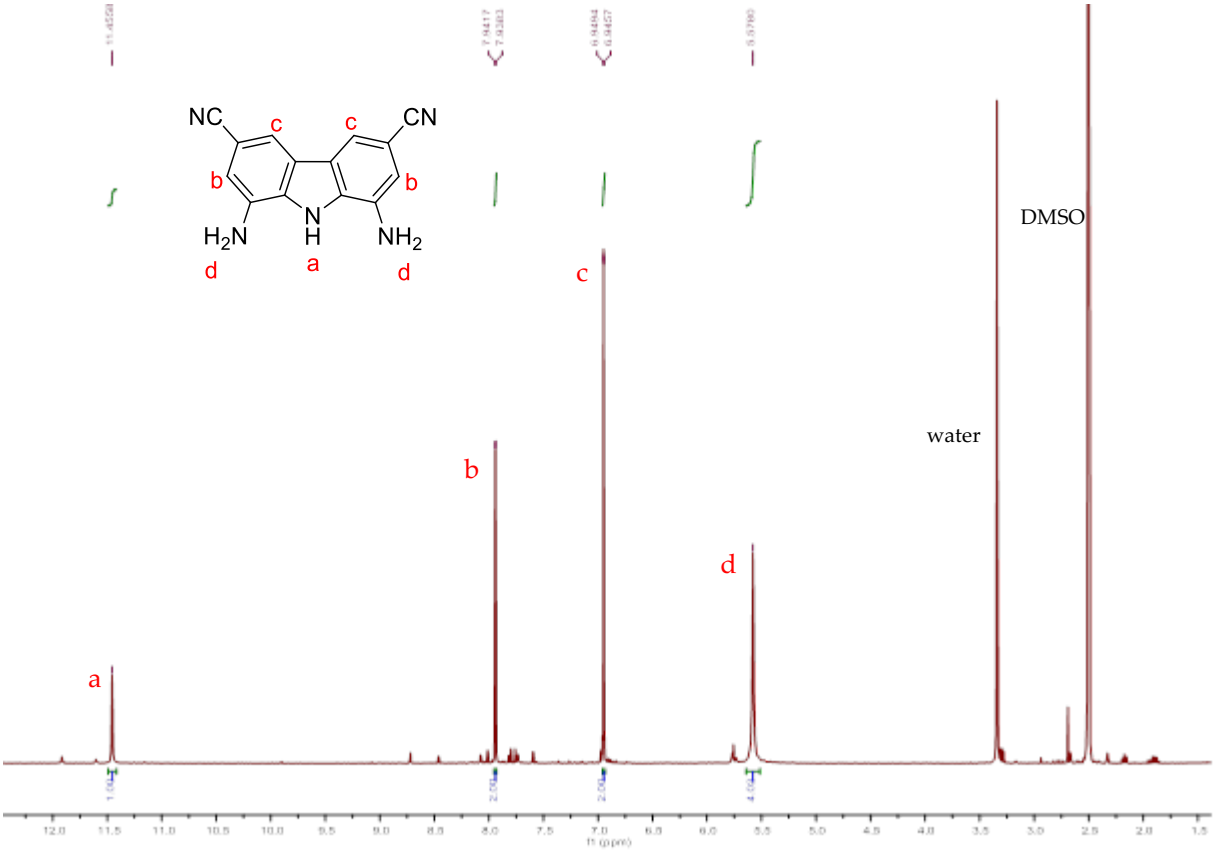

Figure S3. ^{1}H NMR spectrum of 1,8-diamino-3,6-dicyjanocarbazole in DMSO-d_6.

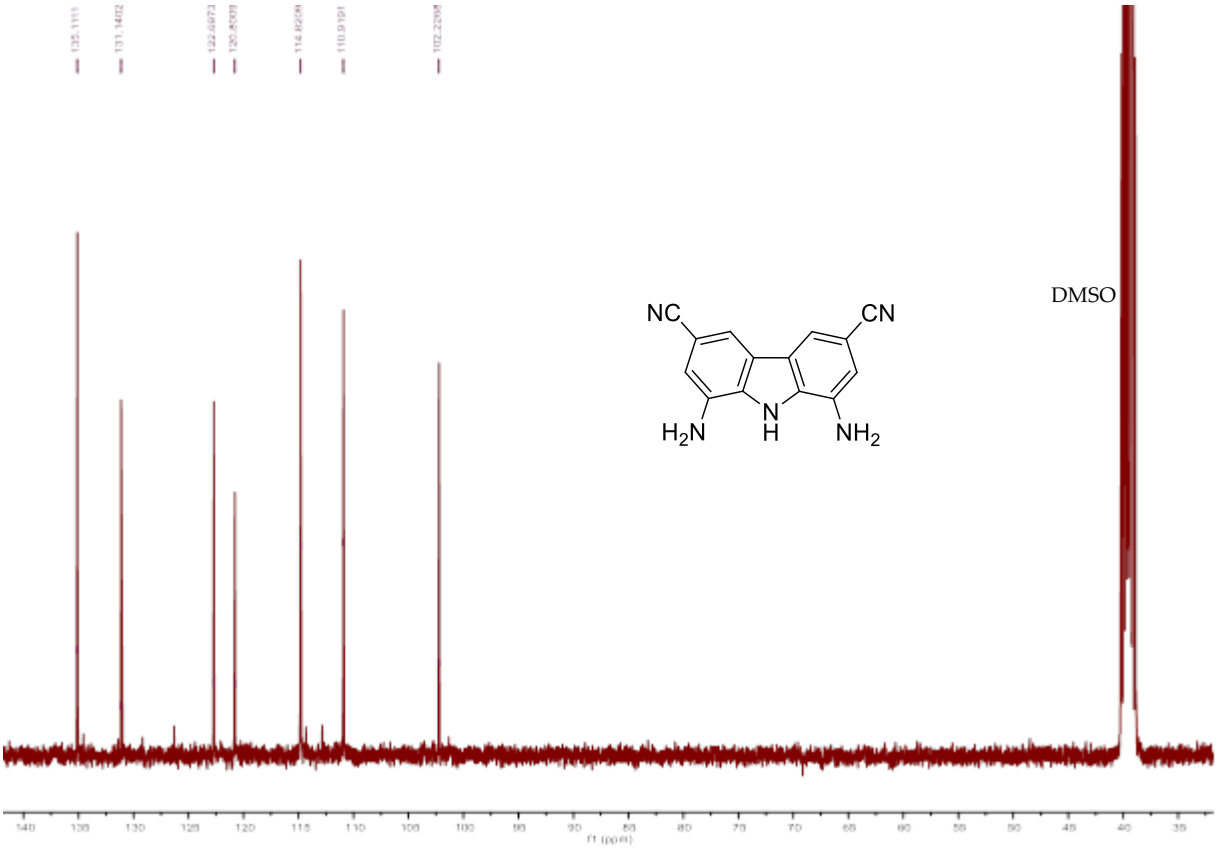

Figure S4. ^{13}C NMR spectrum of 1,8-diamino-3,6-dicyjanocarbazole in DMSO-d_6.

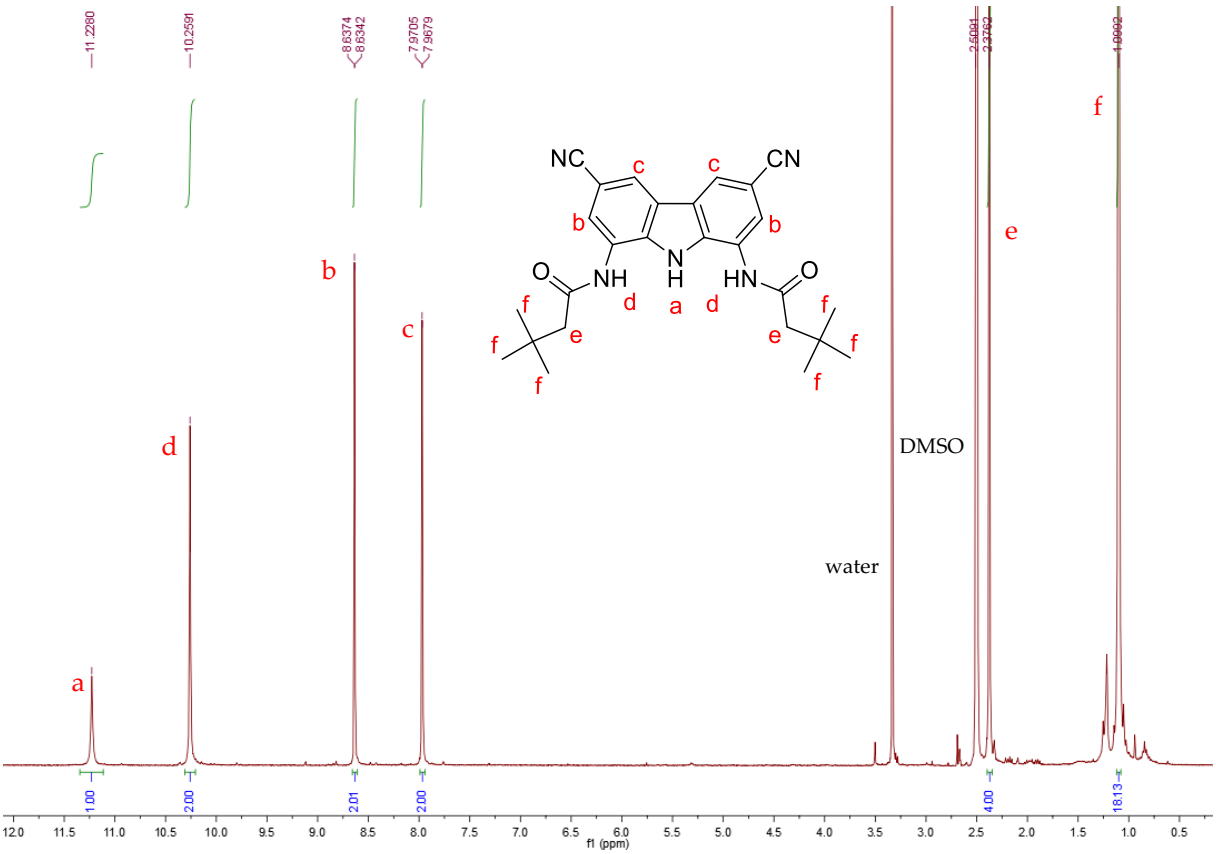

Figure S5. ^{1}H NMR spectrum of **3** in DMSO-d_6.

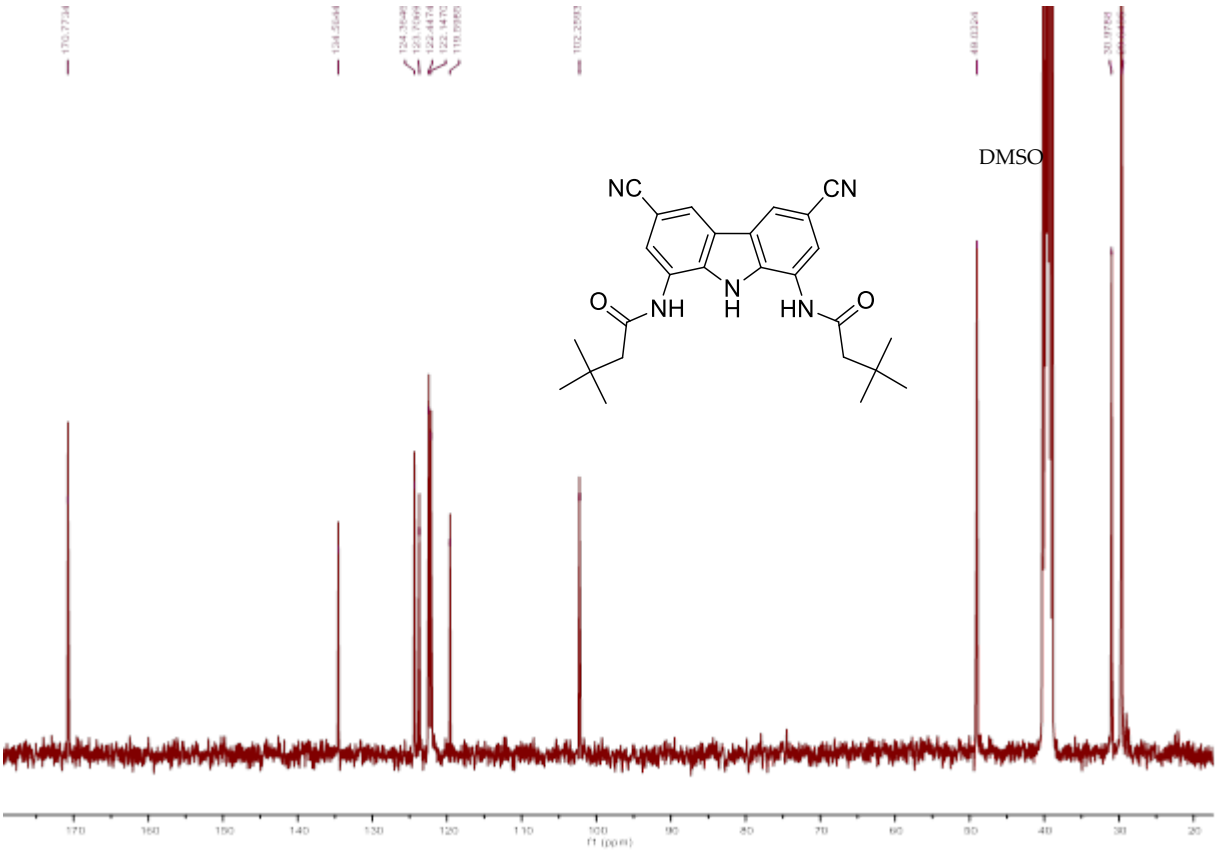

Figure S6. ^{13}C NMR spectrum of **3** in DMSO-d_6.

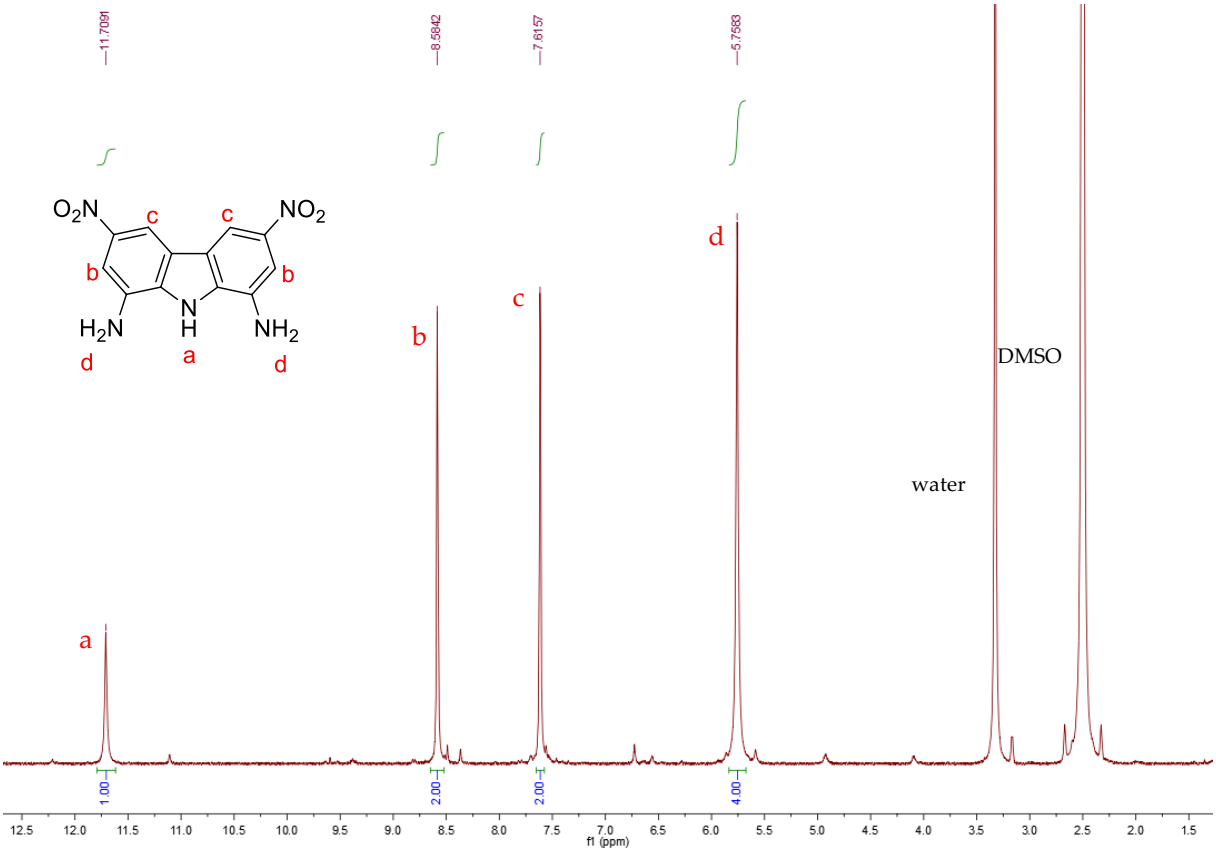

Figure S7. ^{1}H NMR spectrum of 1,8-diamino-3,6-dinitrocarbazole in DMSO-d_6.

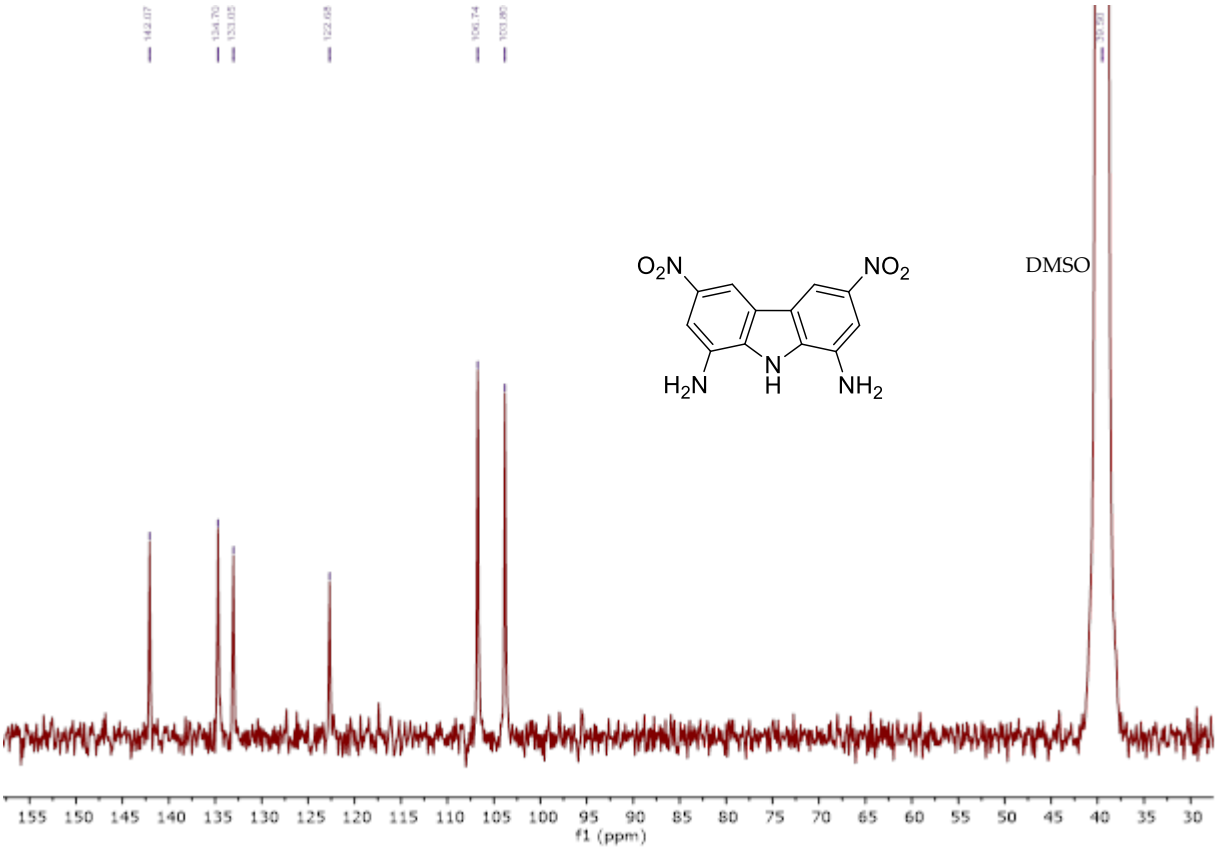

Figure S8. ^{13}C NMR spectrum of 1,8-diamino-3,6-dinitrocarbazole in DMSO-d_6.

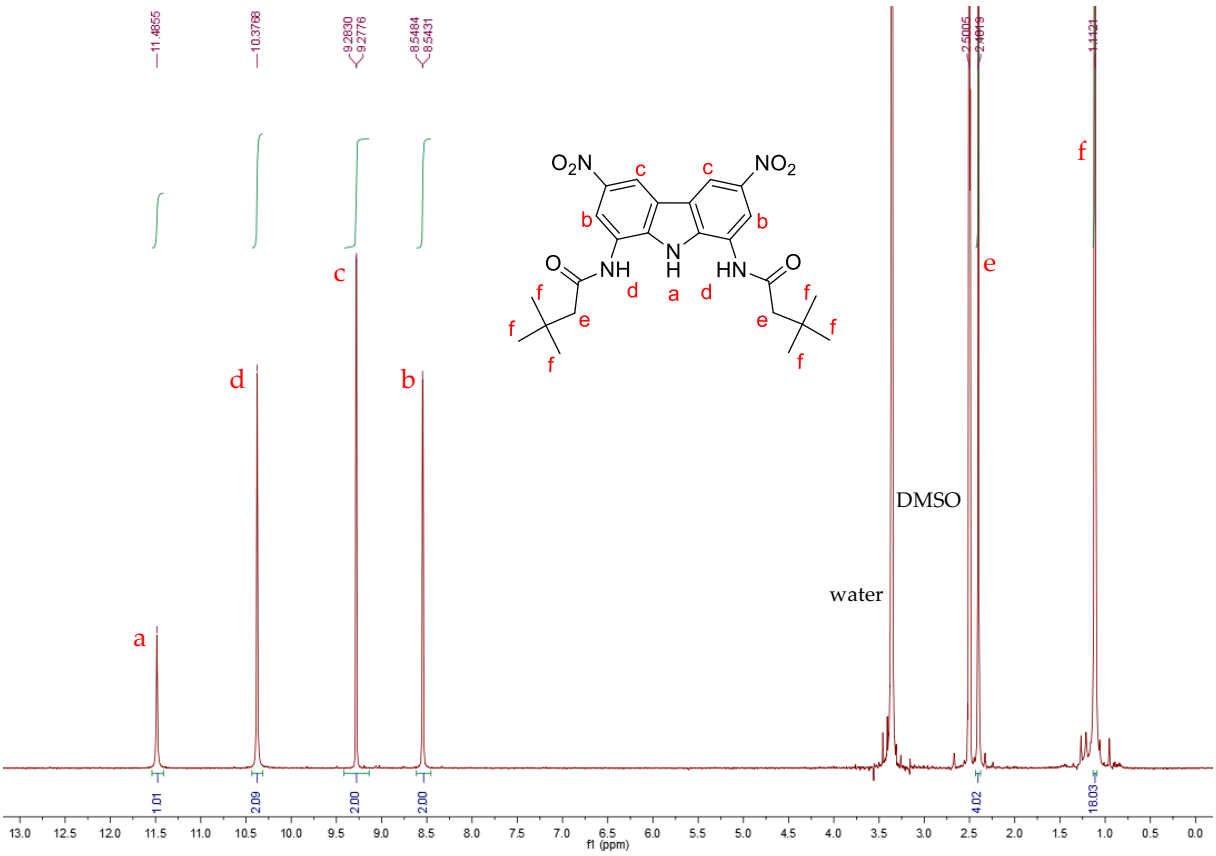

Figure S9. ^{1}H NMR spectrum of **4** in DMSO-d_6.

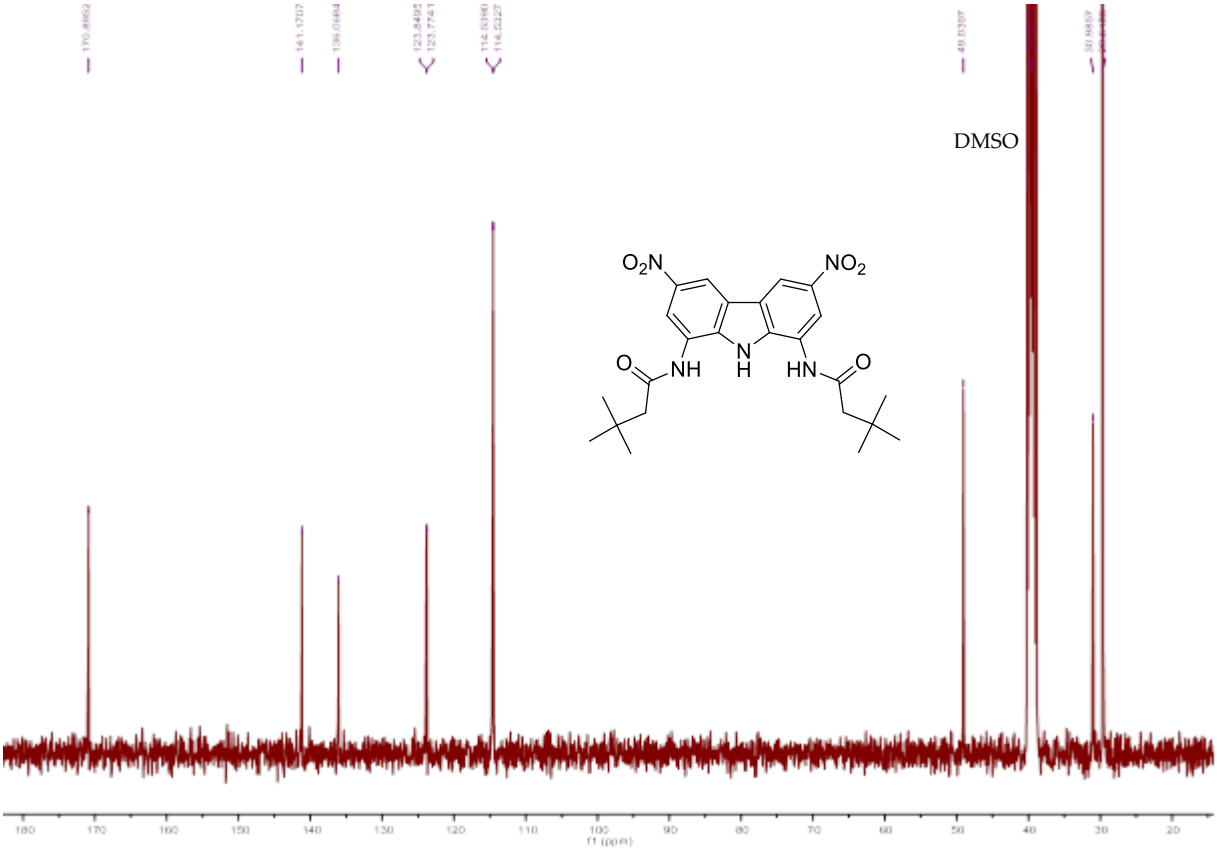

Figure S10. ^{13}C NMR spectrum of **4** in DMSO-d_6.

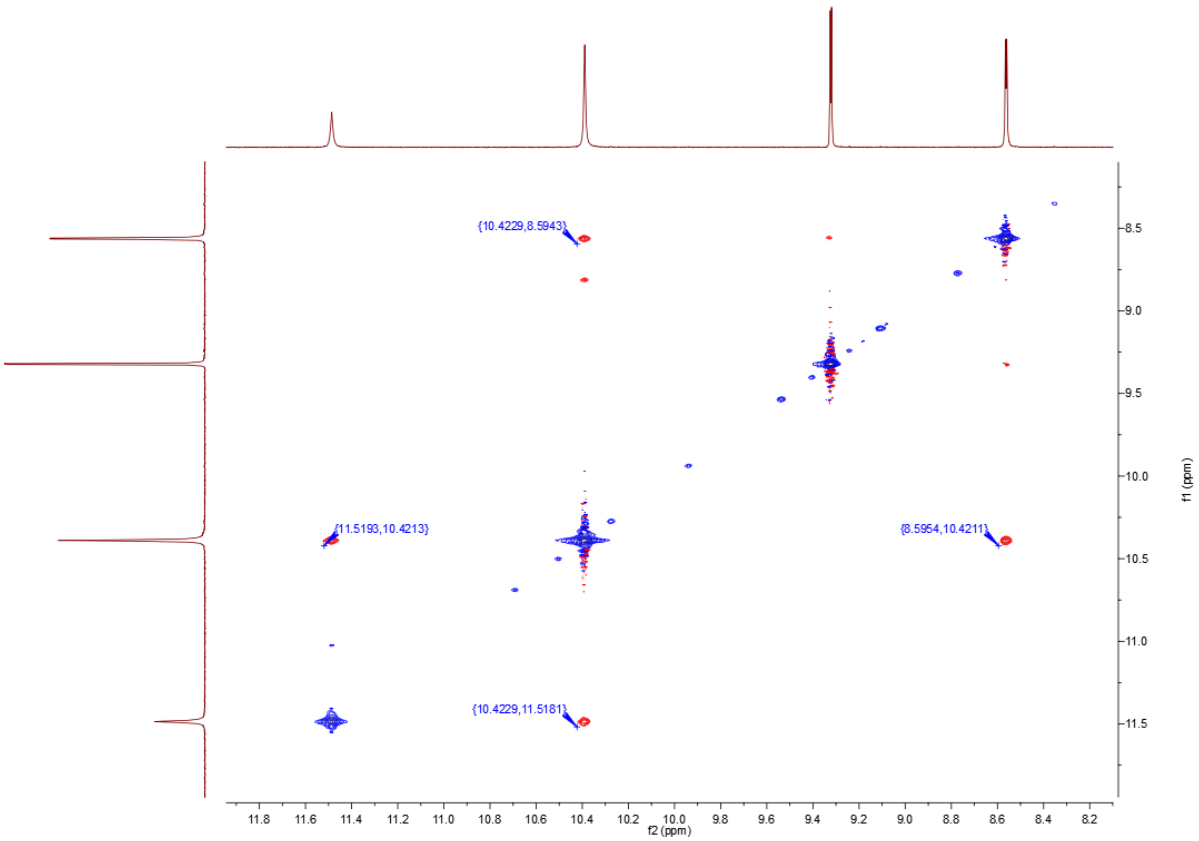

Figure S11. ^{1}H ROESY spectrum of **4** in DMSO-d_6.

2D ROESY (*Rotation Frame Nuclear Overhauser Effect Spectroscopy*) spectrum reveals which hydrogen atoms of **4** are close to each other in space. The protons of the amide groups interact with both carbazole proton NH at 11.52 ppm and CH2/7 protons at 8.60 ppm, what means that both *syn* and *anti*-conformations of the amide groups are populated in DMSO solution, as shown on Scheme S1.

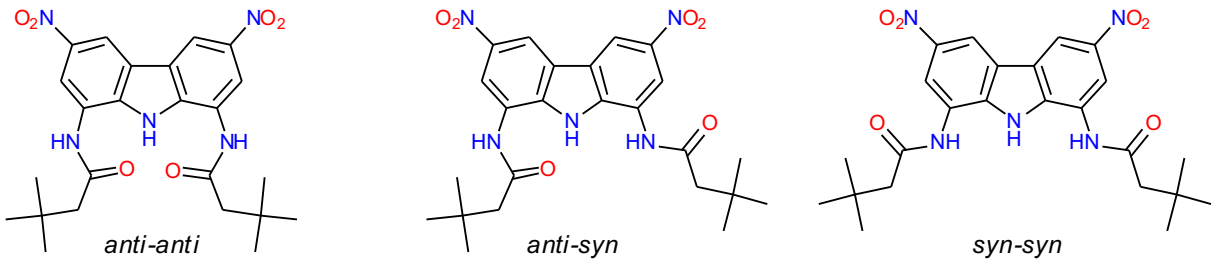

Scheme S1. Amide groups conformations in **4**.

2 Binding studies

2.1 Anion binding studies of receptor **3**

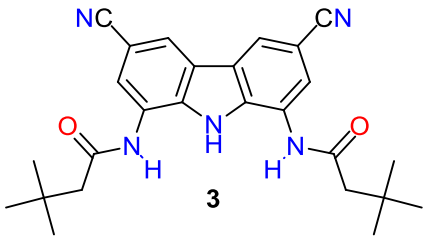

2.1.1 ^{1}H NMR titration of **3** with Cl^- in DMSO/0.5%H_2O

^{1}H NMR titration of 0.01 M solution of receptor **3** in $DMSO_{-d6}$/0.5% H_2O with 0.3 M solution of TBACl (dissolved in the solution of receptor **3**).

a) ^{1}H NMR spectra

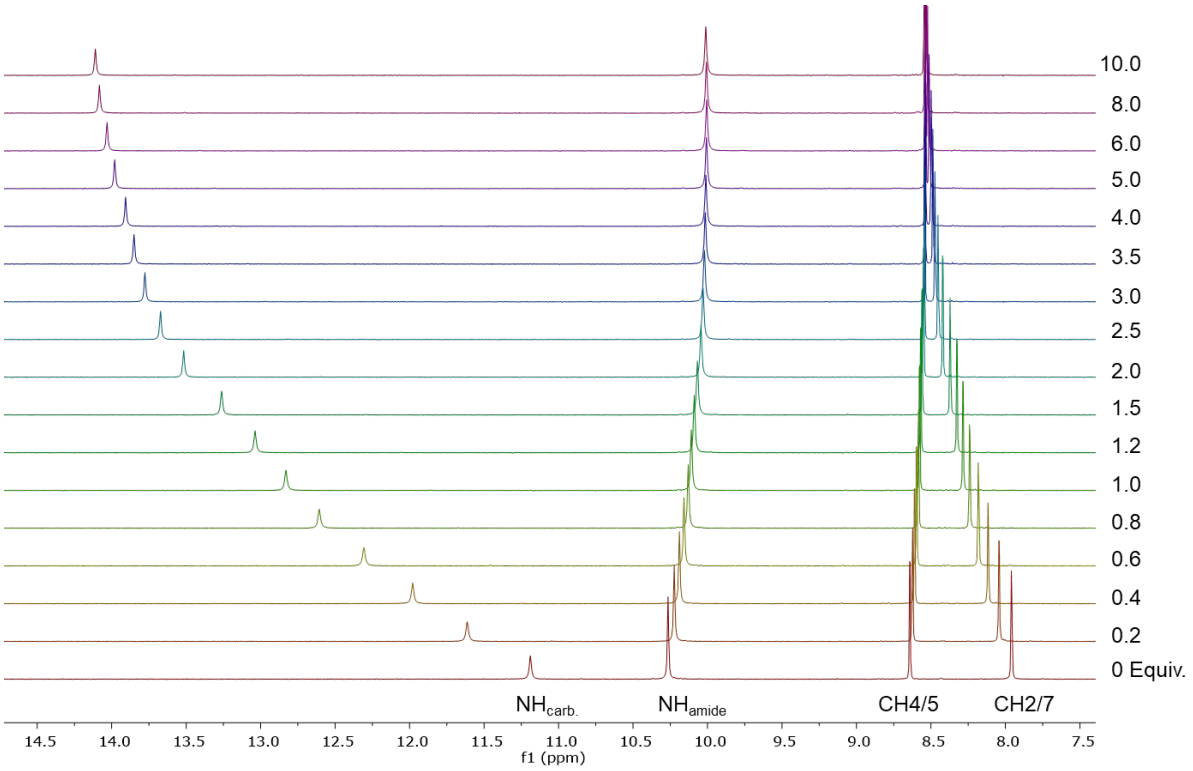

b) Raw data

Added volume of titrant [µL]	Equivalents of TBACl	Chemical shift [ppm]	
		$NH_{carb.}$	NH_{amide}
0.00	0	11.4867	10.3867
4.00	0.2	11.7219	10.3584
8.00	0.4	11.9426	10.3328
16.25	0.6	12.3577	10.2793
25.00	0.8	12.7551	10.2315
33.75	1.0	13.0694	10.1919
42.75	1.2	13.3287	10.1604
52.25	1.5	13.5376	10.1350
66.75	2.0	13.7653	10.1074
91.75	2.5	13.9954	10.0795
120.00	3.0	14.1334	10.0631
150.00	3.5	14.2170	10.0537
182.50	4.0	14.2728	10.0477
218.25	5.0	14.3128	10.0438
300.00	6.0	14.3676	10.0416
400.00	8.0	14.3982	10.0387
686.00	9.0	14.4319	10.0397
911.00	10.0	14.4402	10.0409

c) Titration curves of $NH_{carb.}$ and NH_{amide} protons

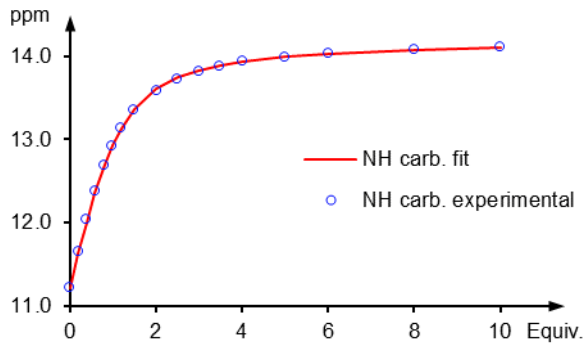

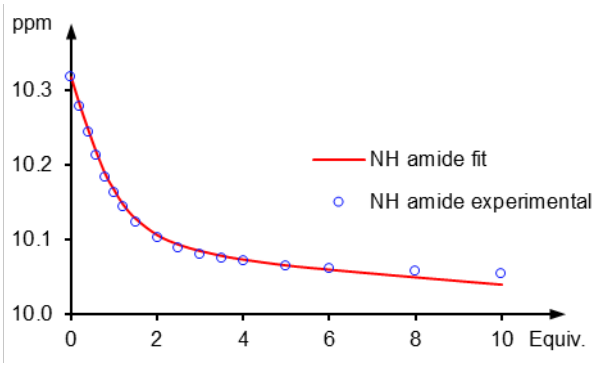

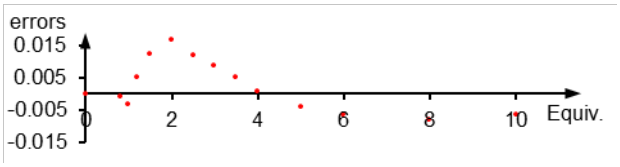

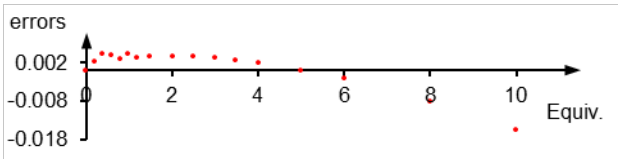

d) Logarithm of the binding constant log K derived from simultaneous fitting of 1:1 model to two selected protons using Bindfit:

log K: 2.497

e) Logarithm of binding constant log K derived from the experiment repeated according to the same methodology:

log K: 2.491

f) Logarithm of binding constant log K averaged from the two experiments:

log K: 2.494

2.1.2 UV-Vis titration of **3** with $H_2PO_4^-$ in DMSO/0.5%H_2O

UV-Vis titration of 1×10^{-4} M solution of receptor **3** in DMSO/0.5% H_2O with 0.0075 M solution of $TBAH_2PO_4$ (dissolved in the solution of receptor **3**).

a) UV-Vis spectra

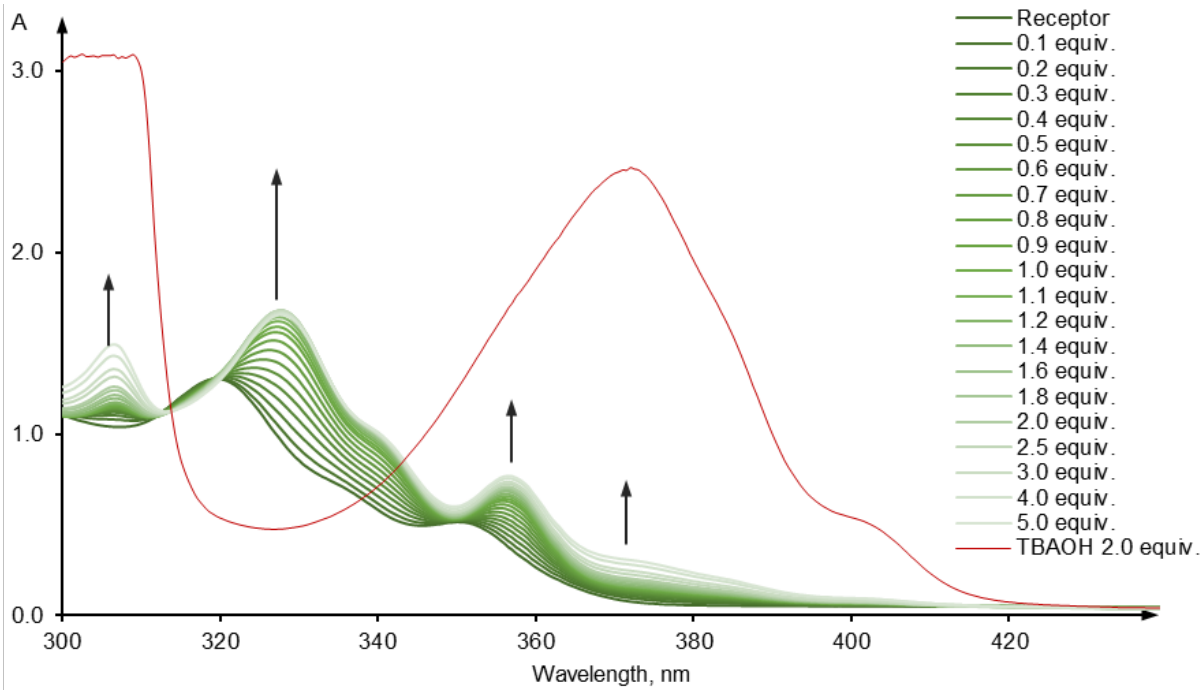

b) Raw data

Equivalents of $TBAH_2PO_4$	307 nm	328 nm	337.5 nm	357 nm	372 nm
0.0	1.038	0.948	0.655	0.361	0.075
0.1	1.080	1.015	0.693	0.398	0.098
0.2	1.101	1.088	0.733	0.431	0.109
0.3	1.117	1.163	0.772	0.460	0.117
0.4	1.128	1.238	0.813	0.491	0.124
0.5	1.137	1.309	0.852	0.520	0.131
0.6	1.143	1.377	0.890	0.548	0.136
0.7	1.147	1.446	0.926	0.576	0.141
0.8	1.149	1.506	0.960	0.600	0.145
0.9	1.155	1.554	0.988	0.621	0.150
1.0	1.159	1.589	1.007	0.637	0.154
1.1	1.166	1.617	1.025	0.651	0.159
1.2	1.175	1.642	1.040	0.664	0.165
1.4	1.195	1.663	1.054	0.679	0.175
1.6	1.218	1.677	1.064	0.693	0.187
1.8	1.242	1.682	1.070	0.702	0.197
2.0	1.262	1.683	1.073	0.709	0.206
2.5	1.314	1.681	1.077	0.724	0.229
3.0	1.358	1.677	1.080	0.737	0.250
4.0	1.430	1.670	1.082	0.754	0.279
5.0	1.491	1.661	1.083	0.768	0.305

c) Titration curves at 337.5 nm.

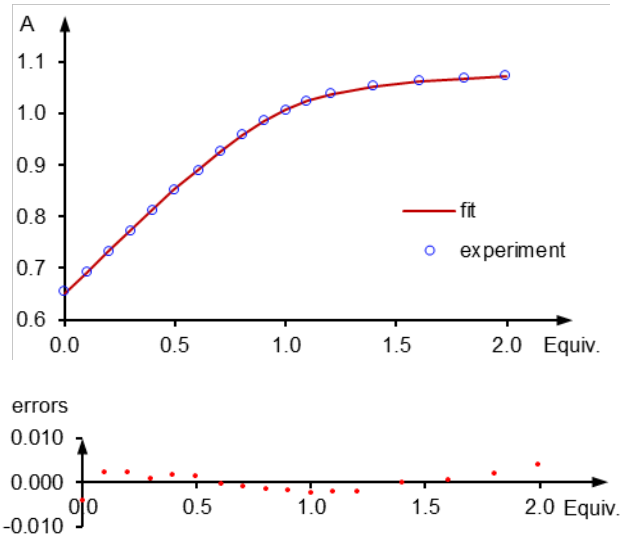

d) Logarithm of the binding constant log K derived from simultaneous fitting of 1:1 model to three selected wavelengths using HypSpec:

log K: 5.370

2.1.3 UV-Vis titration of **3** with $PhCOO^-$ in DMSO/0.5%H_2O

UV-Vis titration of 1×10^{-4} M solution of receptor **3** in DMSO/0.5% H_2O with 0.0075 M solution of TBAPhCOO (dissolved in the solution of receptor **3**).

a) UV-Vis spectra

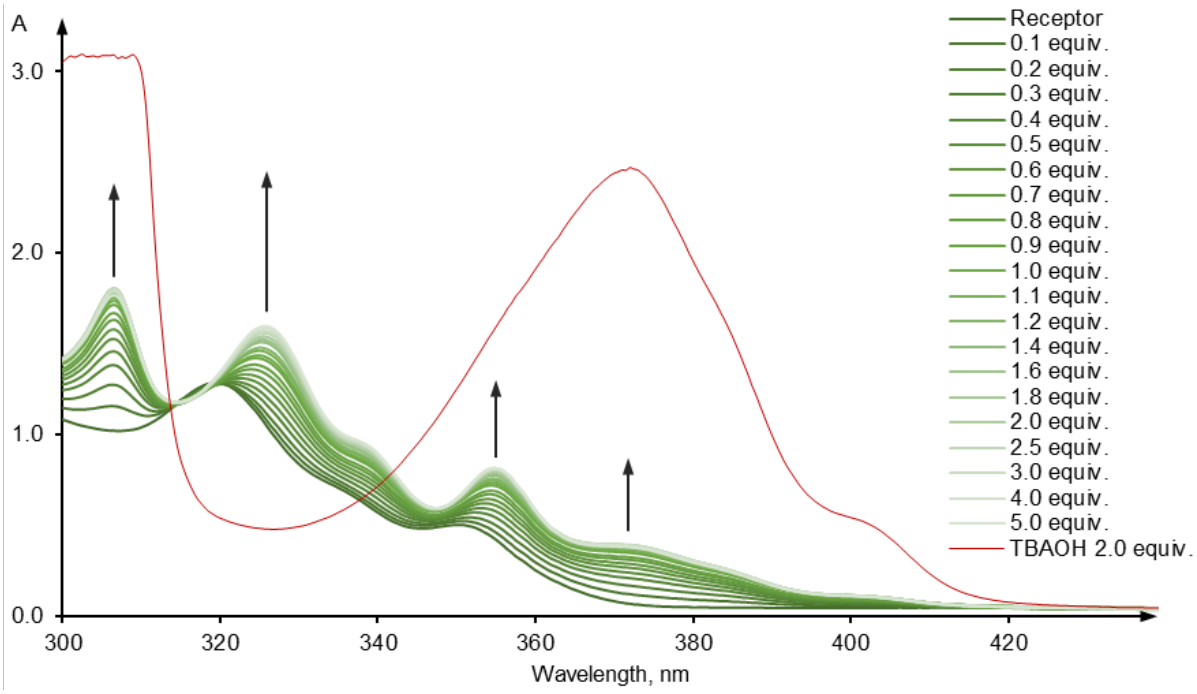

b) Raw data

Equivalents of TBAPhCOO	307 nm	326 nm	357 nm	372 nm
0.0	1.022	1.046	0.349	0.065
0.1	1.154	1.074	0.393	0.119
0.2	1.274	1.113	0.438	0.167
0.3	1.376	1.158	0.480	0.207
0.4	1.453	1.204	0.518	0.239
0.5	1.520	1.248	0.552	0.265
0.6	1.573	1.289	0.581	0.288
0.7	1.627	1.331	0.611	0.310
0.8	1.661	1.363	0.633	0.325
0.9	1.706	1.404	0.662	0.349
1.0	1.733	1.426	0.677	0.359
1.1	1.743	1.450	0.689	0.365
1.2	1.758	1.471	0.704	0.372
1.4	1.772	1.502	0.718	0.379
1.6	1.786	1.521	0.733	0.385
1.8	1.795	1.534	0.741	0.390
2.0	1.798	1.537	0.739	0.389
2.5	1.798	1.558	0.752	0.391
3.0	1.791	1.570	0.756	0.388
4.0	1.782	1.586	0.759	0.386
5.0	1.763	1.599	0.760	0.379

2.1.4 UV-Vis titration of **3** with OH^- in DMSO/0.5%H_2O

UV-Vis titration of 1×10^{-4} M solution of receptor **3** in DMSO/0.5% H_2O with 0.0075 M solution of TBAOH (dissolved in the solution of receptor **3**).

a) UV-Vis spectra

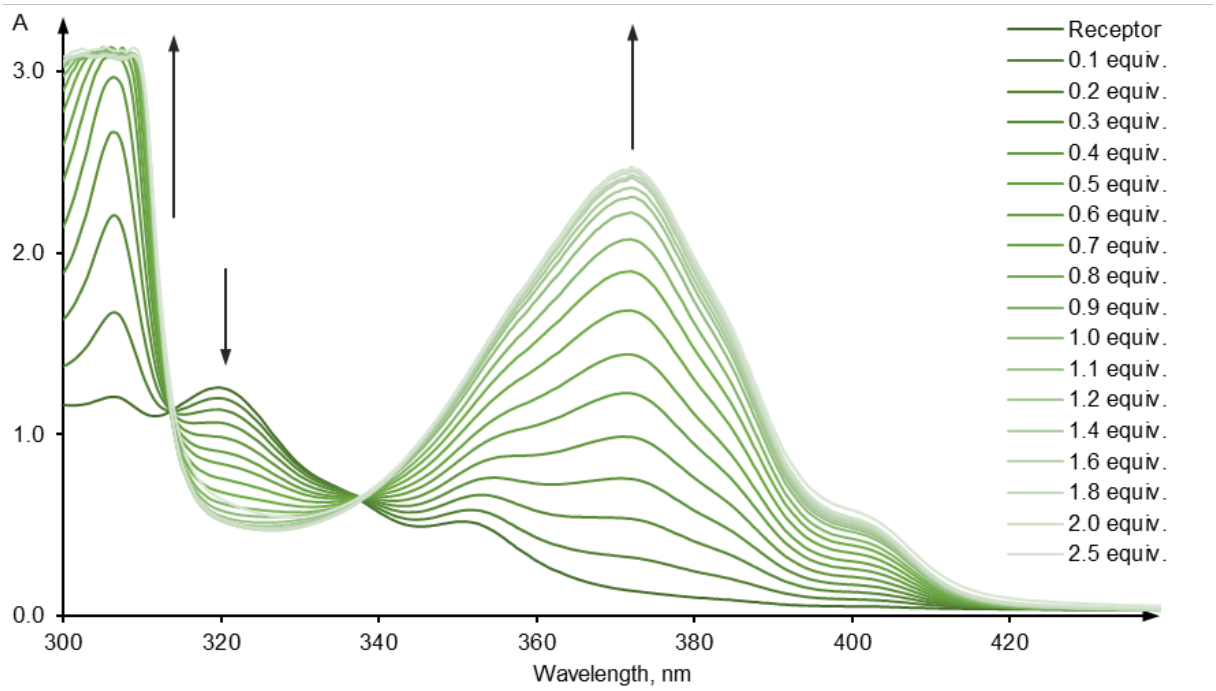

b) Raw data

Equivalents of TBAOH	307 nm	320 nm	350 nm	372 nm
0.0	1.202	1.254	0.520	0.141
0.1	1.667	1.201	0.575	0.321
0.2	2.188	1.133	0.639	0.533
0.3	2.648	1.063	0.706	0.753
0.4	2.955	0.986	0.777	0.987
0.5	3.081	0.906	0.850	1.227
0.6	3.102	0.838	0.915	1.439
0.7	3.105	0.758	0.989	1.682
0.8	3.096	0.685	1.058	1.900
0.9	3.094	0.625	1.115	2.078
1.0	3.082	0.579	1.161	2.220
1.1	3.102	0.549	1.192	2.307
1.2	3.076	0.534	1.209	2.360
1.4	3.080	0.526	1.224	2.414
1.6	3.073	0.527	1.231	2.433
1.8	3.065	0.532	1.242	2.454
2.0	3.074	0.535	1.248	2.471
2.5	3.110	0.646	1.247	2.469

2.2 Anion binding studies of receptor **4**

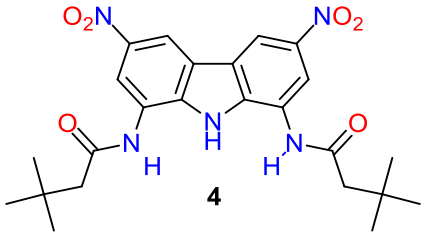

4

2.2.1 ^{1}H NMR titration of **4** with Cl^- in DMSO/0.5%H_2O

^{1}H NMR titration of 0.01 M solution of receptor **4** in $DMSO_{-d6}$/0.5% H_2O with 0.3 M solution of TBACl (dissolved in the solution of receptor **4**).

a) ^{1}H NMR spectra

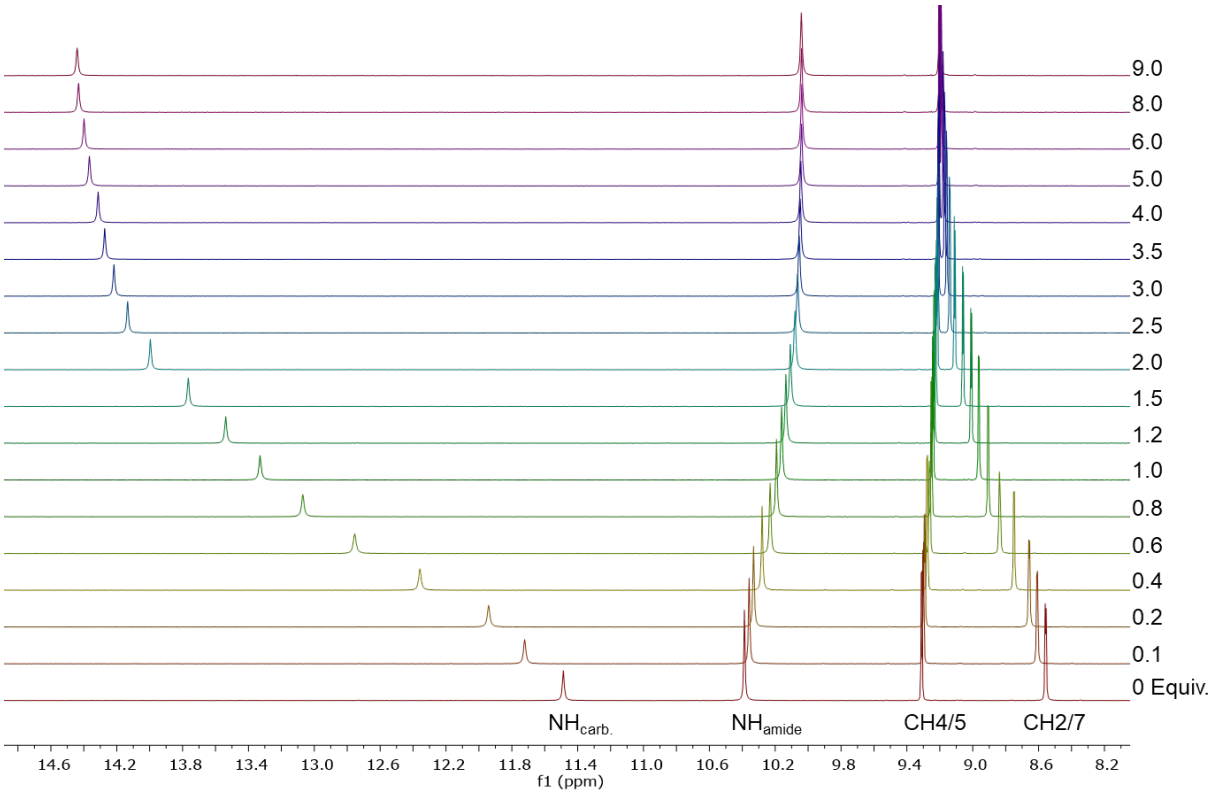

b) Raw data

Added volume of titrant [µL]	Equivalents of TBACl	Chemical shift [ppm]	
		$NH_{carb.}$	NH_{amide}
0.00	0	11.4867	10.3867
4.00	0.1	11.7219	10.3584
8.00	0.2	11.9426	10.3328
16.25	0.4	12.3577	10.2793
25.00	0.6	12.7551	10.2315
33.75	0.8	13.0694	10.1919
42.75	1.0	13.3287	10.1604
52.25	1.2	13.5376	10.1350
66.75	1.5	13.7653	10.1074
91.75	2.0	13.9954	10.0795
120.00	2.5	14.1334	10.0631
150.00	3.0	14.2170	10.0537
182.50	3.5	14.2728	10.0477
218.25	4.0	14.3128	10.0438
300.00	5.0	14.3676	10.0416
400.00	6.0	14.3982	10.0387
686.00	8.0	14.4319	10.0397
911.00	9.0	14.4402	10.0409

c) Titration curve of $NH_{carb.}$ and NH_{amide} protons

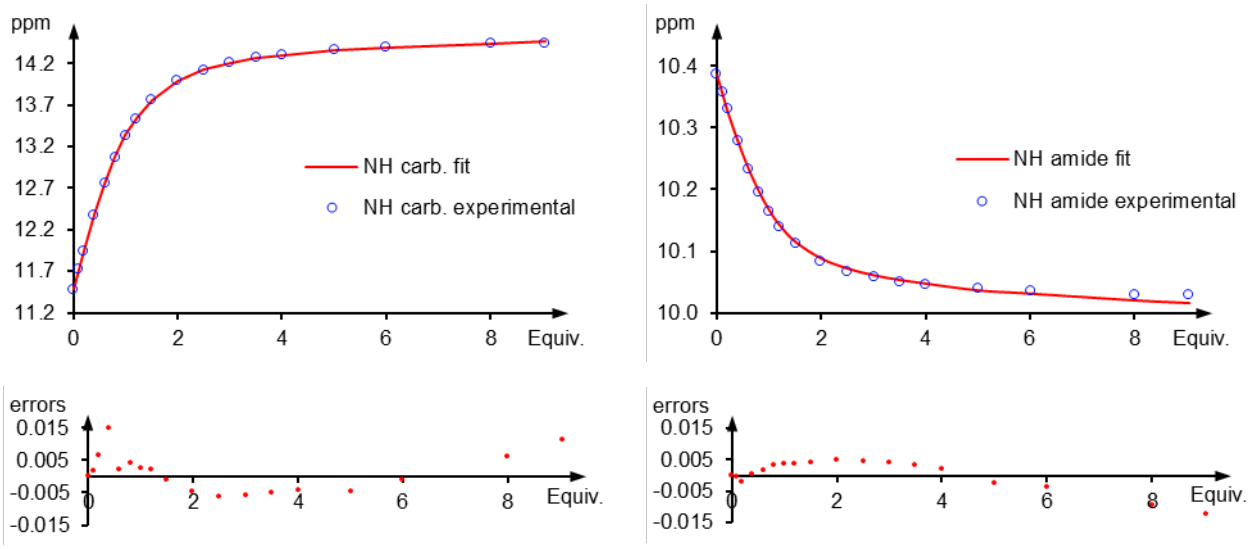

d) Logarithm of the binding constant log K derived from simultaneous fitting of 1:1 model to two selected protons using Bindfit:

log K: 2.584

e) Logarithm of the binding constant log K derived from the experiment repeated according to the same methodology:

log K: 2.491

f) Logarithm of the binding constant log K averaged from the two experiments:

log K: 2.538

2.2.2 UV-Vis titration of **4** with $H_2PO_4^-$ in DMSO/0.5%H_2O

UV-Vis titration of 1×10^{-4} M solution of receptor **4** in DMSO/0.5% H_2O with 0.0075 M solution of $TBAH_2PO_4$ (dissolved in the solution of receptor **4**).

a) UV-Vis spectra

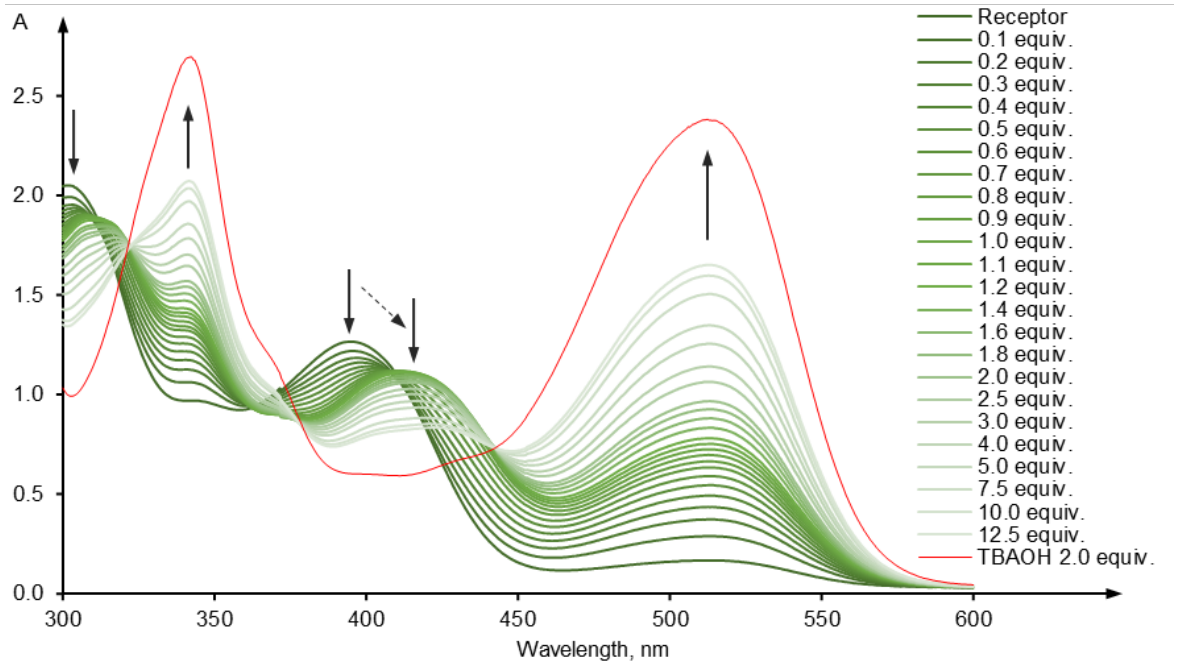

b) Raw data

Equivalents of $TBAH_2PO_4$	343 nm	392 nm	465 nm	513 nm
0.0	0.970	1.261	0.117	0.167
0.1	1.061	1.211	0.183	0.289
0.2	1.123	1.171	0.231	0.373
0.3	1.170	1.140	0.269	0.435
0.4	1.212	1.108	0.305	0.493
0.5	1.249	1.078	0.338	0.545
0.6	1.282	1.050	0.368	0.591
0.7	1.312	1.022	0.397	0.634
0.8	1.331	1.003	0.418	0.665
0.9	1.354	0.986	0.438	0.697
1.0	1.379	0.972	0.455	0.725
1.1	1.398	0.961	0.470	0.752
1.2	1.420	0.952	0.484	0.781
1.4	1.458	0.937	0.509	0.833
1.6	1.495	0.925	0.532	0.881
1.8	1.530	0.914	0.553	0.926
2.0	1.559	0.905	0.572	0.967
2.5	1.635	0.882	0.616	1.064
3.0	1.693	0.863	0.651	1.141
4.0	1.775	0.838	0.702	1.255
5.0	1.848	0.817	0.745	1.348
7.5	1.960	0.781	0.817	1.505
10.0	2.025	0.759	0.861	1.598
12.5	2.064	0.746	0.888	1.652

2.2.3 UV-Vis titration of **4** with $PhCOO^-$ in DMSO/0.5%H_2O

UV-Vis titration of 1×10^{-4} M solution of receptor **4** in DMSO/0.5% H_2O with 0.0075 M solution of TBAPhCOO (dissolved in the solution of receptor **4**).

a) UV-Vis spectra

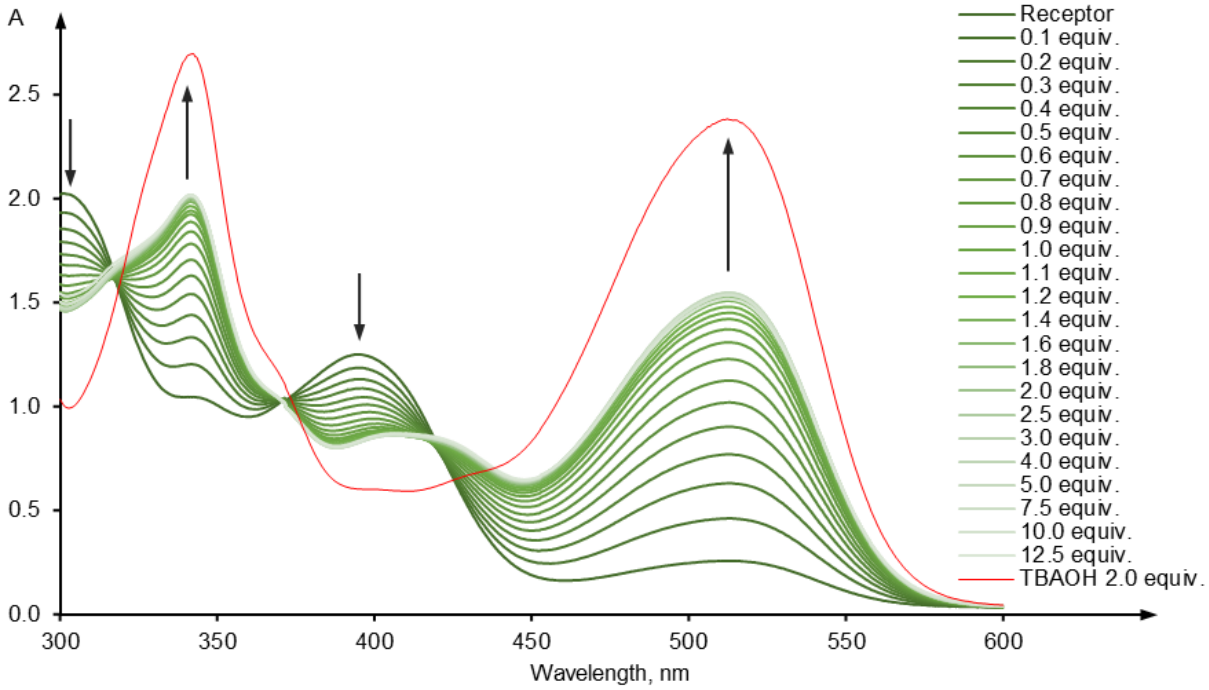

b) Raw data

Equivalents of TBAPhCOO	345 nm	397 nm	450 nm	515 nm
0.0	1.040	1.246	0.189	0.257
0.1	1.189	1.184	0.254	0.460
0.2	1.311	1.130	0.309	0.628
0.3	1.412	1.086	0.356	0.767
0.4	1.509	1.044	0.402	0.900
0.5	1.592	1.008	0.443	1.016
0.6	1.665	0.972	0.480	1.122
0.7	1.737	0.939	0.518	1.225
0.8	1.794	0.912	0.547	1.305
0.9	1.837	0.892	0.571	1.367
1.0	1.871	0.877	0.589	1.416
1.1	1.889	0.868	0.601	1.447
1.2	1.910	0.858	0.613	1.475
1.4	1.930	0.849	0.624	1.504
1.6	1.942	0.844	0.631	1.520
1.8	1.947	0.841	0.635	1.528
2.0	1.947	0.841	0.635	1.528
2.5	1.952	0.842	0.639	1.535
3.0	1.957	0.839	0.642	1.540
4.0	1.960	0.837	0.644	1.543
5.0	1.961	0.837	0.646	1.543
7.5	1.961	0.839	0.648	1.532
10.0	1.961	0.839	0.648	1.532
12.5	1.960	0.846	0.652	1.512

2.2.4 UV-Vis titration of **4** with Cl^- in DMSO/0.5%H_2O

UV-Vis titration of 2×10^{-4} M solution of receptor **4** in DMSO/0.5% H_2O with 0.090 M solution of TBACl (dissolved in the solution of receptor **4**).

a) UV-Vis spectra

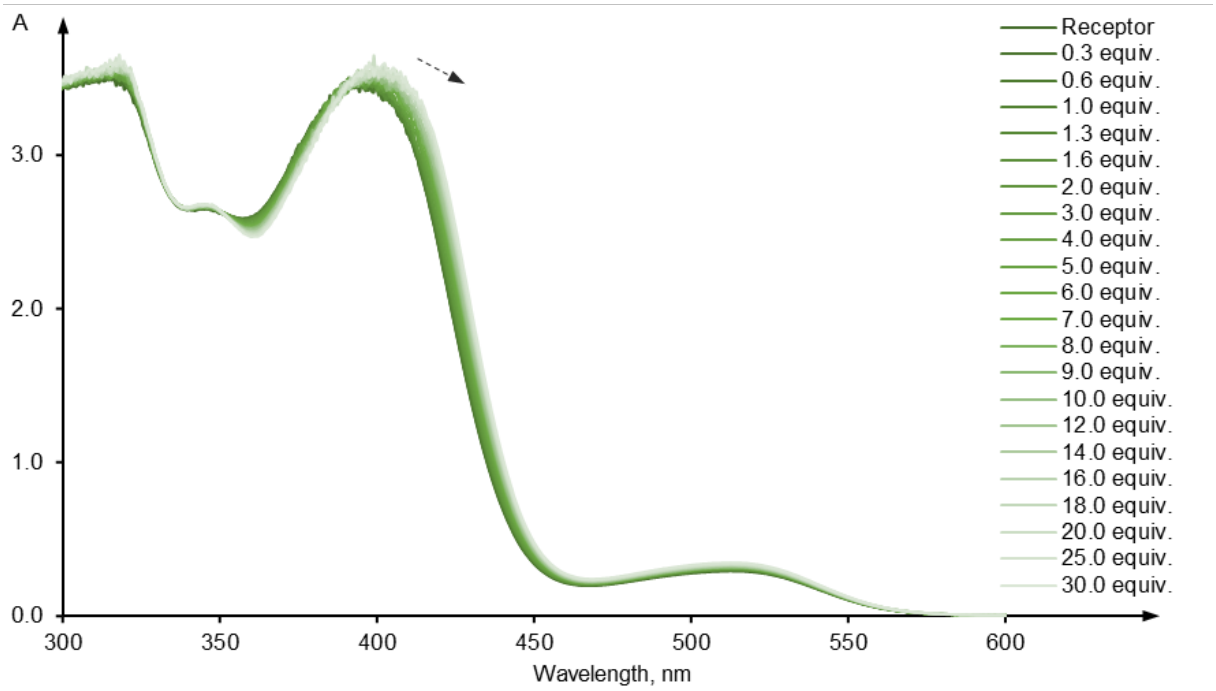

b) Raw data

Equivalents of TBACl	361 nm	430 nm	515 nm
0.0	2.603	1.393	0.291
0.3	2.608	1.403	0.297
0.6	2.606	1.409	0.298
1.0	2.602	1.430	0.300
1.3	2.597	1.455	0.302
1.6	2.597	1.469	0.303
2.0	2.594	1.488	0.305
3.0	2.585	1.516	0.306
4.0	2.572	1.566	0.309
5.0	2.560	1.607	0.310
6.0	2.552	1.647	0.313
7.0	2.543	1.686	0.315
8.0	2.534	1.714	0.315
9.0	2.530	1.742	0.317
10.0	2.519	1.768	0.320
12.0	2.514	1.794	0.322
14.0	2.507	1.835	0.325
16.0	2.499	1.872	0.330
18.0	2.493	1.901	0.333
20.0	2.483	1.927	0.335
25.0	2.480	1.949	0.339
30.0	2.470	1.995	0.346

2.2.5 UV-Vis titration of **4** with OH^- in DMSO/0.5%H_2O

UV-Vis titration of 1×10^{-4} M solution of receptor **4** in DMSO/0.5% H_2O with 0.0075 M solution of TBAOH (dissolved in the solution of receptor **4**).

a) UV-Vis spectra

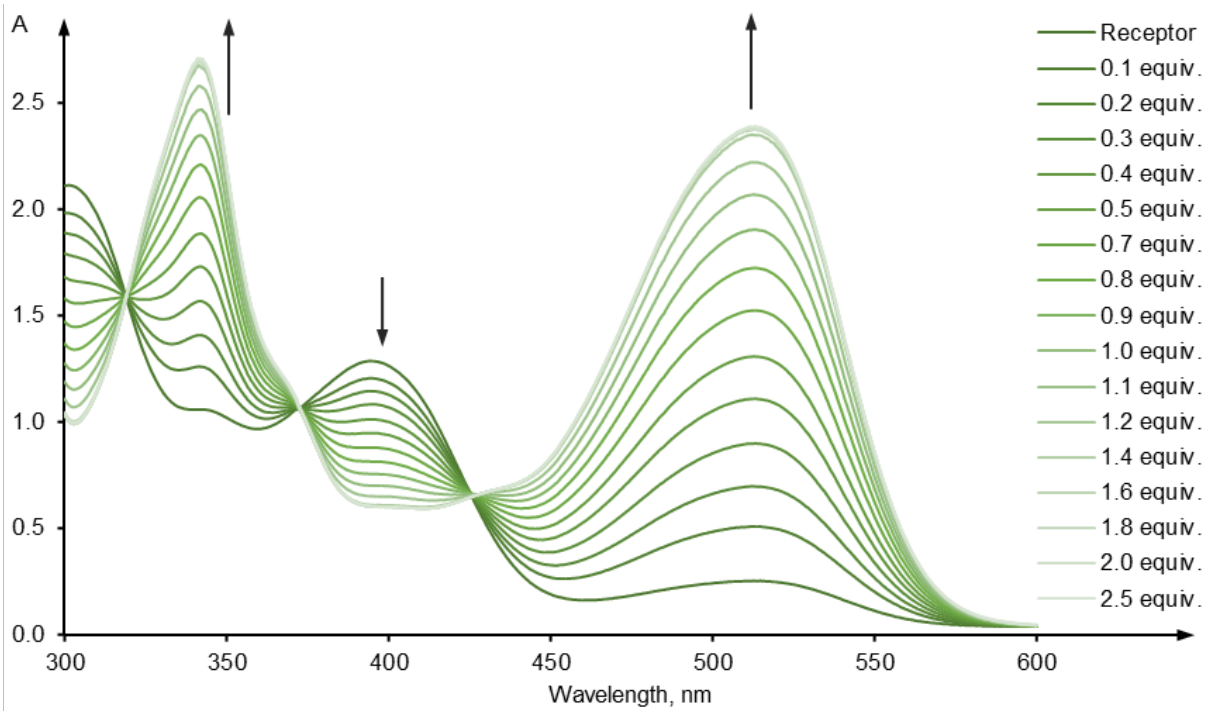

b) Raw data

Equivalents of TBAOH	346 nm	396 nm	450 nm	515 nm
0.0	1.049	1.285	0.190	0.253
0.1	1.231	1.204	0.269	0.508
0.2	1.367	1.144	0.327	0.696
0.3	1.515	1.083	0.388	0.897
0.4	1.662	1.012	0.452	1.107
0.5	1.805	0.948	0.512	1.305
0.6	1.806	0.948	0.512	1.307
0.7	1.961	0.880	0.576	1.522
0.8	2.103	0.814	0.636	1.720
0.9	2.228	0.756	0.690	1.901
1.0	2.340	0.701	0.739	2.064
1.1	2.441	0.650	0.784	2.216
1.2	2.528	0.609	0.823	2.346
1.4	2.550	0.602	0.830	2.372
1.6	2.552	0.602	0.831	2.376
1.8	2.553	0.602	0.831	2.374
2.0	2.554	0.602	0.832	2.377
2.5	2.566	0.604	0.834	2.386

3 Self-dissociation reversal studies

3.1 Self-dissociation reversal studies of receptor **3**

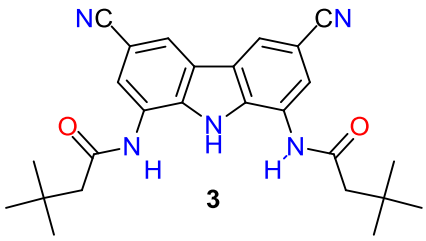

UV-Vis titration of 1×10^{-4} M solution of receptor **3** in DMSO/0.5% H_2O with 0.0075 M solution of TfOH (dissolved in the solution of receptor **3**).

a) UV-Vis spectra

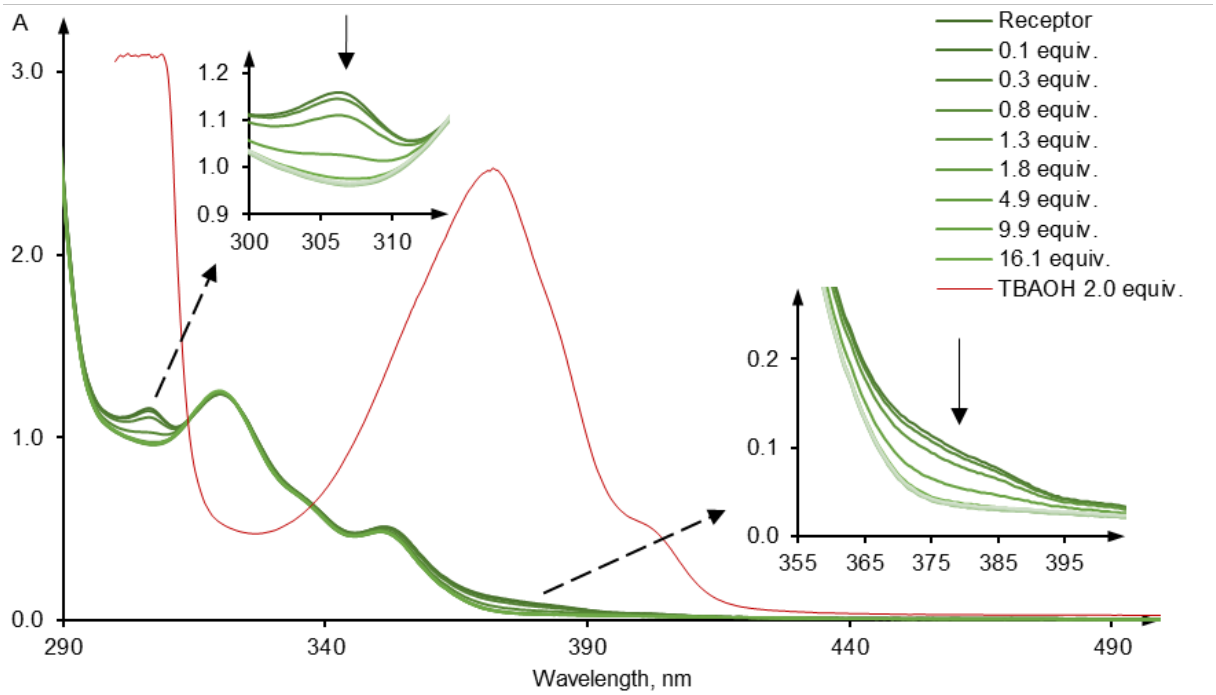

b) Titration curves

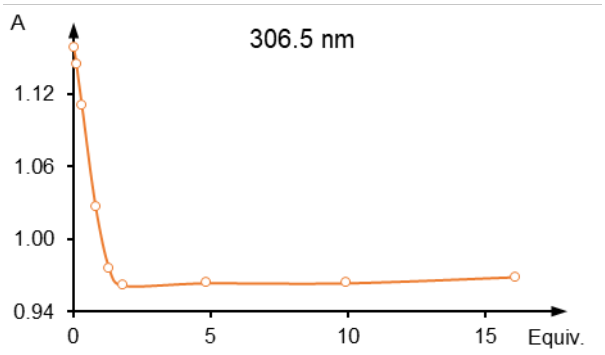

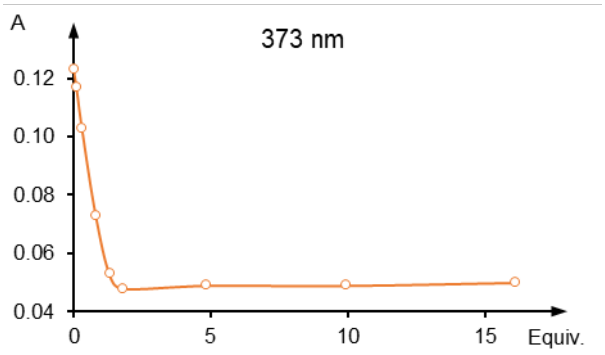

3.2 Self-dissociation reversal studies of receptor **4**

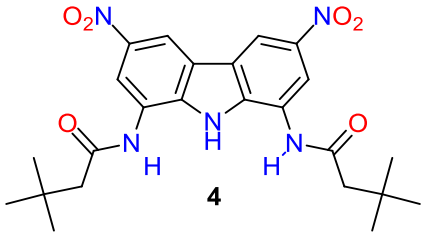

4

UV-Vis titration of 1×10^{-4} M solution of receptor **4** in DMSO/0.5% H_2O with 0.0075 M solution of TfOH (dissolved in the solution of receptor **4**).

a) UV-Vis spectra

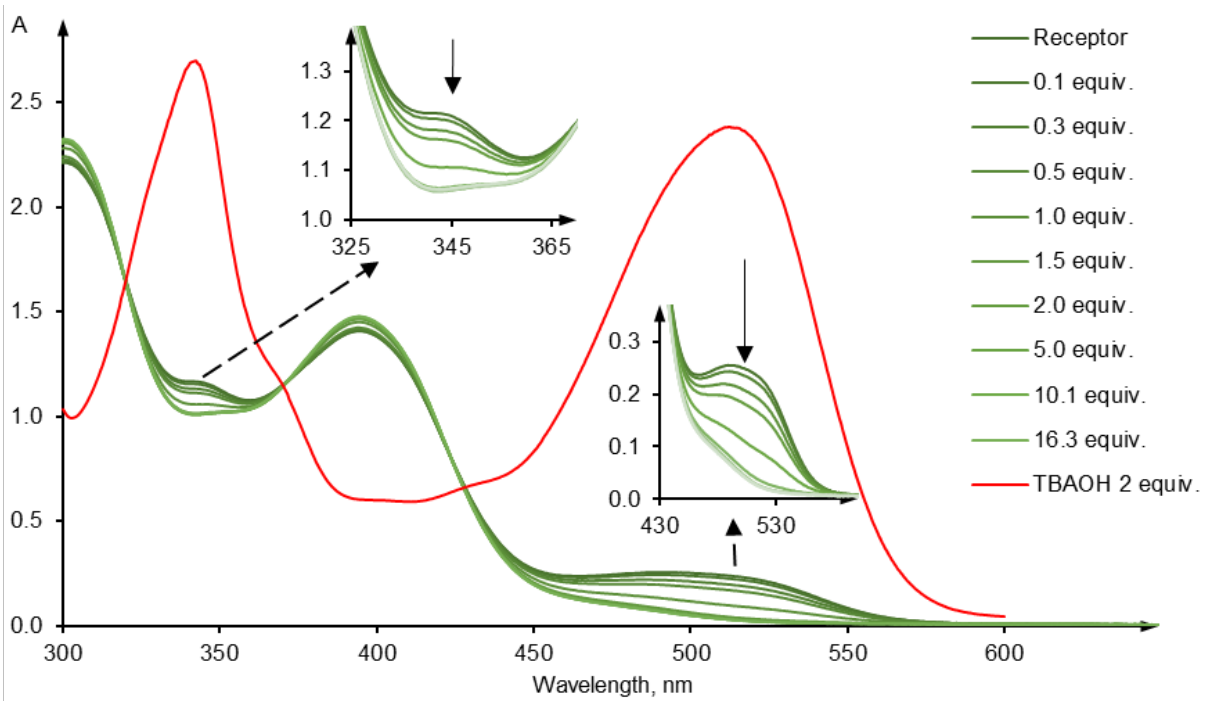

b) Titration curves

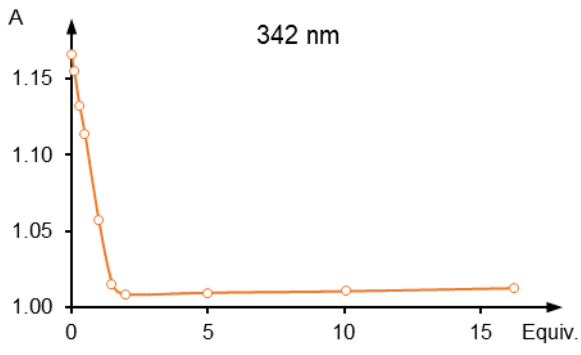

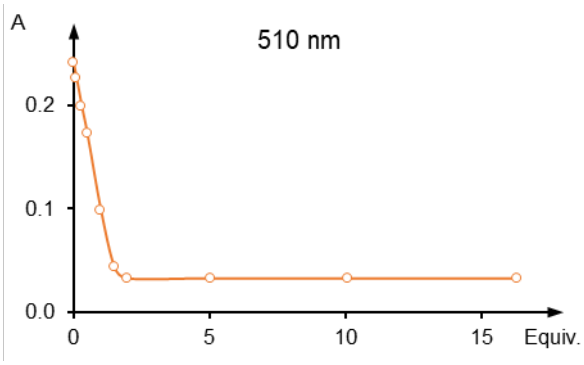

4 Crystallographic data and refinement details

Table S1. Crystal data and structure refinement for investigated compounds.

Identification code	**K3 (3)**	**K4 (4)**
CCDC deposition number	2074344	2074345
Empirical formula	$C_{110}H_{122}Cl_2N_{10}O_4P_2$	$C_{53}H_{61}ClN_5O_6P$
Formula weight	1781.01	930.48
Temperature/K	200.00(10)	200(2)
Crystal system	triclinic	triclinic
Space group	P-*1*	P-*1*
a/Å	11.2744(6)	11.1012(3)
b/Å	14.0732(8)	14.3129(5)
c/Å	16.9993(10)	17.1970(5)
α/°	72.779(5)	72.560(3)
β/°	84.390(5)	84.207(2)
γ/°	78.038(5)	76.749(3)
Volume/Å^3	2518.5(3)	2535.90(14)
Z	1	2
ρ_{calc} g/cm^3	1.174	1.219
μ/mm^{-1}	0.153	0.160
F(000)	948.0	988.0
Crystal size/mm^3	0.201×0.104×0.069	0.959×0.216×0.152
Radiation	MoKα (*λ* = 0.71073)	Mo*Kα* (*λ* = 0.71073)
2*Θ* range for data collection/°	4.482 to 52.742	4.326 to 52.744
Index ranges	-14 ≤ *h* ≤ 14, -17 ≤ k ≤ 17, -21 ≤ l ≤ 21	-13 ≤ *h* ≤ 13, -17 ≤ *k* ≤ 17, -21 ≤ *l* ≤ 21
Reflections collected	37975	42264
Independent reflections	10274 [R_{int} = 0.0651, R_{sigma} = 0.0784]	10365 [R_{int} = 0.0334, R_{sigma} = 0.0309]
Data/restraints/parameters	10274/30/633	10365/1/603
Goodness-of-fit on F^2	1.020	1.067
Final *R* indexes [*I*>=2*σ* (*I*)]	R_1 = 0.0643, wR_2 = 0.1226	R_1 = 0.0538, wR_2 = 0.1317
Final *R* indexes [all data]	R_1 = 0.1168, wR_2 = 0.1434	R_1 = 0.0688, wR_2 = 0.1401
Largest diff. peak/hole/e Å^{-3}	0.23/-0.25	0.51/-0.41

Table S2. Bond lengths for complex with **3**.

Atom	Atom	Length/Å	Atom	Atom	Length/Å
C2A	C3A	1.413(4)	C20	C25	1.388(4)
C2A	C7A	1.396(4)	C20	P19	1.794(3)
C2A	N1A	1.373(3)	C21	C22	1.376(4)
C2B	C3B	1.407(4)	C22	C23	1.377(4)
C2B	C7B	1.402(4)	C23	C24	1.380(4)
C2B	N1A	1.369(3)	C24	C25	1.377(4)
C3A	C3B	1.442(4)	C26	C27	1.392(4)
C3A	C4A	1.398(4)	C26	C31	1.390(4)
C3B	C4B	1.392(4)	C26	P19	1.788(3)
C4A	C5A	1.382(4)	C27	C28	1.383(4)
C4B	C5B	1.383(4)	C28	C29	1.374(4)
C5A	C6A	1.406(4)	C29	C30	1.376(4)
C5A	C15A	1.445(4)	C30	C31	1.384(4)
C5B	C6B	1.409(4)	C32	C33	1.383(4)
C5B	C15B	1.443(4)	C32	C37	1.386(4)
C6A	C7A	1.385(4)	C32	P19	1.789(3)
C6B	C7B	1.387(4)	C33	C34	1.382(4)
C7A	N8A	1.403(3)	C34	C35	1.360(5)
C7B	N8B	1.407(3)	C35	C36	1.369(5)
C9A	C10A	1.501(4)	C36	C37	1.382(5)
C9A	N8A	1.369(3)	C38	C39	1.393(4)
C9A	O17A	1.218(3)	C38	C43	1.393(4)
C9B	C10B	1.508(4)	C38	P19	1.789(3)
C9B	N8B	1.366(3)	C39	C40	1.379(4)
C9B	O17B	1.218(3)	C40	C41	1.377(5)
C10A	C11A	1.535(4)	C41	C42	1.371(4)
C10B	C11B	1.544(4)	C42	C43	1.385(4)
C11A	C12A	1.524(5)	C44B	C45B	1.388(10)
C11A	C13A	1.530(4)	C45B	C46B	1.387(11)
C11A	C14A	1.514(5)	C46B	C47B	1.397(11)
C11B	C12B	1.522(4)	C47B	C48B	1.406(11)
C11B	C13B	1.532(4)	C44A	C45A	1.379(13)
C11B	C14B	1.522(4)	C45A	C46A	1.376(14)
C15A	N16A	1.137(4)	C46A	C47A	1.382(14)
C15B	N16B	1.141(3)	C47A	C48A	1.384(13)
C20	C21	1.392(4)			

Table S3. Valence angles for complex with **3**.

Atom	Atom	Atom	Angle/˚	Atom	Atom	Atom	Angle/˚
C7A	C2A	C3A	123.3(2)	N16B	C15B	C5B	179.7(4)
N1A	C2A	C3A	108.8(2)	C2B	N1A	C2A	109.1(2)
N1A	C2A	C7A	127.9(2)	C9A	N8A	C7A	127.6(2)
C7B	C2B	C3B	122.9(2)	C9B	N8B	C7B	127.9(2)
N1A	C2B	C3B	109.5(2)	C21	C20	P19	120.3(2)
N1A	C2B	C7B	127.6(2)	C25	C20	C21	119.3(3)
C2A	C3A	C3B	106.5(2)	C25	C20	P19	120.3(2)
C4A	C3A	C2A	119.2(3)	C22	C21	C20	120.1(3)
C4A	C3A	C3B	134.3(3)	C21	C22	C23	120.2(3)
C2B	C3B	C3A	106.1(2)	C22	C23	C24	120.1(3)
C4B	C3B	C2B	119.8(3)	C25	C24	C23	120.1(3)
C4B	C3B	C3A	134.1(3)	C24	C25	C20	120.1(3)
C5A	C4A	C3A	117.6(3)	C27	C26	P19	119.6(2)
C5B	C4B	C3B	117.1(3)	C31	C26	C27	119.6(3)
C4A	C5A	C6A	122.7(3)	C31	C26	P19	120.8(2)
C4A	C5A	C15A	120.8(3)	C28	C27	C26	119.5(3)
C6A	C5A	C15A	116.6(3)	C29	C28	C27	120.7(3)
C4B	C5B	C6B	123.3(2)	C28	C29	C30	120.1(3)
C4B	C5B	C15B	119.3(3)	C29	C30	C31	120.1(3)
C6B	C5B	C15B	117.4(3)	C30	C31	C26	120.0(3)
C7A	C6A	C5A	120.8(3)	C33	C32	C37	119.3(3)
C7B	C6B	C5B	120.0(3)	C33	C32	P19	119.5(2)
C2A	C7A	N8A	118.3(2)	C37	C32	P19	120.9(2)
C6A	C7A	C2A	116.5(2)	C34	C33	C32	120.4(3)
C6A	C7A	N8A	125.2(3)	C35	C34	C33	119.7(3)
C2B	C7B	N8B	118.3(2)	C34	C35	C36	120.8(3)
C6B	C7B	C2B	116.8(2)	C35	C36	C37	120.2(3)
C6B	C7B	N8B	124.9(2)	C36	C37	C32	119.6(3)
N8A	C9A	C10A	114.1(2)	C39	C38	P19	119.6(2)
O17A	C9A	C10A	123.1(3)	C43	C38	C39	119.5(3)
O17A	C9A	N8A	122.8(3)	C43	C38	P19	120.8(2)
N8B	C9B	C10B	114.6(2)	C40	C39	C38	120.0(3)
O17B	C9B	C10B	122.9(3)	C41	C40	C39	120.2(3)
O17B	C9B	N8B	122.5(3)	C42	C41	C40	120.3(3)
C9A	C10A	C11A	115.3(2)	C41	C42	C43	120.6(3)
C9B	C10B	C11B	115.6(2)	C42	C43	C38	119.5(3)
C12A	C11A	C10A	110.8(3)	C26	P19	C20	109.55(12)

C12A	C11A	C13A	109.0(3)	C26	P19	C32	109.36(13)
C13A	C11A	C10A	106.6(3)	C26	P19	C38	111.53(13)
C14A	C11A	C10A	110.2(3)	C32	P19	C20	108.10(13)
C14A	C11A	C12A	109.6(3)	C32	P19	C38	109.30(12)
C14A	C11A	C13A	110.6(3)	C38	P19	C20	108.93(13)
C12B	C11B	C10B	111.4(2)	C46B	C45B	C44B	127.2(15)
C12B	C11B	C13B	109.7(3)	C45B	C46B	C47B	133.3(15)
C13B	C11B	C10B	106.7(2)	C46B	C47B	C48B	124.4(13)
C14B	C11B	C10B	110.0(2)	C46A	C45A	C44A	133(2)
C14B	C11B	C12B	109.2(3)	C45A	C46A	C47A	165(3)
C14B	C11B	C13B	109.8(3)	C46A	C47A	C48A	132(3)
N16A	C15A	C5A	177.9(3)				

Table S4. Bond lengths for complex with **4**.

Atom	Atom	Length/Å	Atom	Atom	Length/Å
N1A	C2A	1.372(3)	N15B	O16B	1.218(3)
N1A	C2B	1.374(3)	N15B	O17B	1.223(3)
C2A	C3A	1.408(3)	P19	C20	1.786(2)
C2A	C7A	1.407(3)	P19	C26	1.792(2)
C2B	C3B	1.410(3)	P19	C32	1.796(2)
C2B	C7B	1.406(3)	P19	C38	1.793(2)
C3A	C3B	1.446(3)	C20	C21	1.400(3)
C3A	C4A	1.395(3)	C20	C25	1.389(3)
C3B	C4B	1.393(3)	C21	C22	1.383(4)
C4A	C5A	1.378(3)	C22	C23	1.374(4)
C4B	C5B	1.377(3)	C23	C24	1.381(4)
C5A	C6A	1.399(3)	C24	C25	1.379(3)
C5A	N15A	1.464(3)	C26	C27	1.394(3)
C5B	C6B	1.402(3)	C26	C31	1.390(3)
C5B	N15B	1.464(3)	C27	C28	1.385(4)
C6A	C7A	1.384(3)	C28	C29	1.377(4)
C6B	C7B	1.385(3)	C29	C30	1.375(4)
C7A	N8A	1.405(3)	C30	C31	1.389(4)
C7B	N8B	1.406(3)	C32	C33	1.399(3)
N8A	C9A	1.371(3)	C32	C37	1.395(3)
N8B	C9B	1.368(3)	C33	C34	1.377(3)
C9A	C10A	1.502(3)	C34	C35	1.383(4)
C9A	O18A	1.222(3)	C35	C36	1.386(4)
C9B	C10B	1.510(3)	C36	C37	1.382(3)
C9B	O18B	1.218(3)	C38	C39	1.387(3)
C10A	C11A	1.541(4)	C38	C43	1.391(3)
C10B	C11B	1.542(3)	C39	C40	1.389(4)
C11A	C12A	1.525(4)	C40	C41	1.368(5)
C11A	C13A	1.532(4)	C41	C42	1.379(5)
C11A	C14A	1.521(4)	C42	C43	1.382(4)
C11B	C12B	1.525(3)	C45	C46	1.337(8)
C11B	C13B	1.529(4)	C46	C47	1.414(8)
C11B	C14B	1.522(4)	C47	C48	1.415(9)
N15A	O16A	1.227(3)	C48	C49	1.359(8)
N15A	O17A	1.228(3)			

Table S5. Valence angles for complex with **4**.

Atom	Atom	Atom	Angle/˚	Atom	Atom	Atom	Angle/˚
C2A	N1A	C2B	108.97(18)	C14B	C11B	C12B	109.2(2)
N1A	C2A	C3A	109.40(18)	C14B	C11B	C13B	110.2(3)
N1A	C2A	C7A	127.9(2)	O16A	N15A	C5A	118.23(19)
C7A	C2A	C3A	122.7(2)	O16A	N15A	O17A	122.8(2)
N1A	C2B	C3B	109.09(18)	O17A	N15A	C5A	118.95(19)
N1A	C2B	C7B	127.8(2)	O16B	N15B	C5B	118.6(2)
C7B	C2B	C3B	123.07(19)	O16B	N15B	O17B	122.5(2)
C2A	C3A	C3B	106.18(19)	O17B	N15B	C5B	118.9(2)
C4A	C3A	C2A	120.12(19)	C20	P19	C26	111.18(11)
C4A	C3A	C3B	133.7(2)	C20	P19	C32	109.26(10)
C2B	C3B	C3A	106.36(18)	C20	P19	C38	109.87(11)
C4B	C3B	C2B	119.8(2)	C26	P19	C32	109.38(10)
C4B	C3B	C3A	133.9(2)	C26	P19	C38	109.42(10)
C5A	C4A	C3A	116.1(2)	C38	P19	C32	107.66(11)
C5B	C4B	C3B	116.3(2)	C21	C20	P19	120.01(18)
C4A	C5A	C6A	124.8(2)	C25	C20	P19	120.40(17)
C4A	C5A	N15A	118.3(2)	C25	C20	C21	119.6(2)
C6A	C5A	N15A	116.92(19)	C22	C21	C20	119.5(2)
C4B	C5B	C6B	124.9(2)	C23	C22	C21	120.4(2)
C4B	C5B	N15B	117.9(2)	C22	C23	C24	120.3(2)
C6B	C5B	N15B	117.23(19)	C25	C24	C23	120.2(2)
C7A	C6A	C5A	119.5(2)	C24	C25	C20	120.0(2)
C7B	C6B	C5B	119.3(2)	C27	C26	P19	119.61(18)
C6A	C7A	C2A	116.8(2)	C31	C26	P19	120.50(19)
C6A	C7A	N8A	124.93(19)	C31	C26	C27	119.7(2)
N8A	C7A	C2A	118.29(19)	C28	C27	C26	120.0(3)
C6B	C7B	C2B	116.7(2)	C29	C28	C27	120.0(3)
C6B	C7B	N8B	125.13(19)	C30	C29	C28	120.4(2)
N8B	C7B	C2B	118.21(19)	C29	C30	C31	120.4(3)
C9A	N8A	C7A	127.63(19)	C30	C31	C26	119.5(3)
C9B	N8B	C7B	128.05(19)	C33	C32	P19	119.62(18)
N8A	C9A	C10A	114.26(19)	C37	C32	P19	120.69(17)
O18A	C9A	N8A	122.7(2)	C37	C32	C33	119.6(2)
O18A	C9A	C10A	123.1(2)	C34	C33	C32	119.9(2)
N8B	C9B	C10B	114.81(19)	C33	C34	C35	120.3(2)
O18B	C9B	N8B	122.4(2)	C34	C35	C36	120.2(2)
O18B	C9B	C10B	122.8(2)	C37	C36	C35	120.1(2)

C9A	C10A	C11A	114.8(2)	C36	C37	C32	119.9(2)
C9B	C10B	C11B	115.8(2)	C39	C38	P19	119.31(19)
C12A	C11A	C10A	111.3(2)	C39	C38	C43	120.0(2)
C12A	C11A	C13A	109.1(2)	C43	C38	P19	120.22(19)
C13A	C11A	C10A	106.4(2)	C38	C39	C40	119.9(3)
C14A	C11A	C10A	110.0(2)	C41	C40	C39	119.8(3)
C14A	C11A	C12A	109.5(3)	C40	C41	C42	120.6(3)
C14A	C11A	C13A	110.5(3)	C41	C42	C43	120.4(3)
C12B	C11B	C10B	111.3(2)	C42	C43	C38	119.2(3)
C12B	C11B	C13B	109.5(3)	C45	C46	C47	130.8(8)
C13B	C11B	C10B	106.0(2)	C48	C47	C46	131.5(7)
C14B	C11B	C10B	110.6(2)	C49	C48	C47	130.3(8)

4.1 ^{1}H NMR of crystallised complex [**4** × Ph_4PCl] dissolved in $CDCl_3$